"Oceanographic and Meteorlogical Research Based on the Data Products of SEASAT"

Semi-Annual Progress Rpeort

March 31, 1983

Grant No. NAGW-266

Professor Willard J. Pierson
Principal Investigator
Institute of Marine and Atmospheric Sciences

The City College
of
The City University of New York
Convent Avenue at 138th Street
New York, N.Y. 10031

DRAFT
PRELIMINARY
LIMITED DISTRIBUTION

SYNOPTIC SCALE WIND FIELD PROPERTIES FROM THE SEASAT SASS

By

Willard J. Pierson, Jr.
Winfield B. Sylvester
Robert E. Salfi

CUNY Institute of Marine and Atmospheric Sciences at
The City College

The City College of the City University of New York

Convent Ave. at 138th St.
New York, NY 10032

Prepared for
The National Aeronautics and Space Administration
Washington, DC.
Contract NAGW-266.

ABSTRACT

Dealiased SEASAT SASS vector winds obtained during the GOASEX program have been processed to obtain superobservations centered on a one degree by one degree grid. The results provide values for the combined effects of mesoscale variability and communication noise on the individual SASS winds. Each grid point of the synoptic field provides the mean synoptic east-west and north-south wind components plus estimates of the standard deviations of these means. These superobservations winds are then processed further to obtain synoptic scale vector winds stress fields, the horizontal divergence of the wind, the curl of the wind stress and the vertical velocity at 200 m above the sea surface, each with appropriate standard deviations for each grid point value. The resulting fields appear to be consistant over large distances and to agree with, for example, geostationary cloud images obtained concurrently. Their quality is far superior to that of analyses based on conventional data.

INTRODUCTION

The ability to determine the winds in the planetary boundary layer over the oceans of the Earth by a radar scatterometer called the SASS on SEASAT has been demonstrated. The objectives of the SASS program were met, and perhaps exceeded, as described by Lame and Born (1982). A problem was identified when it was recognized that errors in the conventional data need to be better understood. The sources for the differences between a SASS-1 winds, a conventionally measured wind, and a wind derived from a planetary boundary layer analysis using conventional data are many and varied. Yet to be produced are planetary boundary layer analyses of the winds based on the SEASAT SASS-1 data only, augmented by a minimum amount of conventional data such as atmospheric pressures at the sea surface and air sea temperature differences. The purpose of this investigation is to prepare and analyse wind fields from the SASS data.

The three most important applications of SEASAT-SASS-like data in the future will be (1) the correct description of the winds over the entire global ocean at an appropriate resolution, (2) the use of these data to produce vastly improved initial value updates for computer based synoptic scale numerical weather predictions and (3) as shown, by O'Brien, et al. (1982), the specification of the wind stress field and the curl of the wind stress at the sea surface for oceanographic applications. In this investigation, synoptic scale vector wind fields with a known error structure will be produced at a one degree resolution from the SEASAT SASS-1 GOASEX data. These synoptic scale wind fields will be used to compute fields for the horizontal divergence of the winds in the planetary boundary, the vertical velocity at 200 meters, and to determine the error structure of the resulting fields. The vector wind stress fields can then be found from the vector wind fields, and the errors in these fields can be computed. Finally, the curl of the wind stress can be computed, with a specified error structure.

Certain assumptions need to be made concerning the accuracy of the present SASS-1 model function and the wind recovery algorithm. Also the drag coefficient that relates wind stress to the wind at ten meters is a matter of some uncertainty. If any of these assumptions need modification and updating

for future systems, the main results of this study will still be applicable.

As a first effort, the atmosphere will be assumed to be neutrally stratified. An application of the Monin-Obukhov theory for non-neutral stability as in Large and Pond (1981) would provide an improved wind field at 19.5 (or 10) meters for the computation of divergence. The field for the air-sea temperature difference would be needed to an accuracy comparable to the neutral stability wind field.

DATA

The data used in this investigation were provided by the NASA Langley Research Center. They consist of the de-aliased SASS-1 vector winds produced as the final product of the analysis of the SASS data for the SEASAT orbit segments chosen for intensive study during the Gulf of Alaska SEASAT Experiment (GOASEX). Preliminary resultss for this experiment are described by Jones, et al. (1979). Two workshop reports, Born, et al. (1979) and Barrick, et al. (1979), plus a summary of conventional data analyses, Woiceshyn (1979) give additional details.

The SASS-1 model function was based on the JASIN data with results summarized by Jones, et al. (1982), Schroeder, et al. (1982) Moore, et al. (1982) and Brown, et al. (1982). As described by Jones, et al. (1982), the GOASEX data were reprecessed by means of the SASS-1 model function. De-aliasing was accomplished by selecting that wind direction closest to the planetary boundary layer wind fields obtained from conventional data. The model function recovers the effective neutral stability wind at 19.5 meters.

The winds recovered from the SASS are very densely concentrated over the swath scanned by that instrument on SEASAT. Examples can be found for the raw data density in Wurtele, et al. (1982). Only pairs of backscatter measurements 90^{o} apart were used to obtain winds with all combinations of vertically (V) and horizontally (H) polarized measurements (i.e. V with V, H with H, V with H and H with V). For this study, no distinction has been made for possible effect of polarization. The communication noise errors could be quite different for the different polarization combinations.

A sample of a data listing for a particular GOASEX pass is shown in Table 1a and 1b. The data for a north bound pass of revolution 1141 are shown. The central part of the full table is repeated in both 1a and 1b.

In order, the values tabulated in the twenty one columns (as numbered with 11, 12 and 13 repeated) are as follows:

(1) Revolution Number,
(2) the latitude of the mid point of the line connecting the centers of the two cells used in the calculation,
(3) the longitude as above,

(4) the wind speed in meters per second from a boundary layer model,
(5) the neutral stability wind speed from the SASS,
(6) the from which wind direction in degree from a boundary layer model clockwise from north,
(7) the closest alias wind direction from the SASS,
(8) a quality code for the accuracy of the boundary layer wind,
(9) a code for the estimate of the precipitation in the area,
(10) the distance between the two SASS cells,
(11) the average of the values in the next two columns,
(12) the incidence angle in degrees of the forward beam,
(13) the incidence angle of the aft beam,
(14) the pointing direction of the forward beam in degrees clockwise from north,
(15) the pointing direction of the aft beam,
(16) the backscatter in decibels measured by the forward beam,
(17) the backscatter for the aft beam,
(18) the noise standard deviation for the forward beam in per cent (multiply the antilog of the backscatter by this number divided by 100 to get the standard deviation of the measurement),
(19) the NSD for the aft beam,
(20) the polarization of the forward beam (0 = H, 1 = V) and
(21) the polarization of the aft beam.

In this investigation, only the elements of the data vector corresponding to LAT, LONG, WSP, WDR and FOR AZ were used to derive the results. For some portions of some of the SASS swaths, the boundary layer conventional winds differed substantially from the SASS winds. The data base for the conventional fields will be discussed later. Future scatterometer systems may eliminate the need to remove aliases as in Pierson and Salfi (1982), for example. Wind fields produced by the methods described herein would then be independent of conventional data sources, except sea surface atmospheric pressure and, perhaps, air temperatures. Sea temperature is remotely sensed and does not vary rapidly.

The GOASEX data set provided by NASA Langley contained the results of the analysis of nine passes over the North Pacific. These were portions of revolutions 825, 826, 1141, 1183, 1212, 1226, 1227, 1298 and 1299. Extensive depictions of conventional data are available for those five orbit segments underlined above (Woiceshyn (1979)).

TABLE 1a, Sample Data Listing from Rev. 1141, Left Side

1 REV NO.	2 LAT	3 LON	4 AWSP	5 WSP	6 AWDR	7 WDR	8 QUAL	9 PRECIP	10 CELL SEP DIST	11 THETA	12 FOR THETA	13 AFT THETA
1141	53.10	207.27	21.5	19.8	278.5	260.2	1	4	24.0	34.60	34.40	34.80
1141	53.14	207.19	21.5	21.5	278.7	284.2	1	4	32.0	34.50	34.40	34.60
1141	53.57	207.26	21.5	19.0	279.3	267.6	1	4	21.0	36.50	34.60	38.40
1141	53.60	207.18	21.5	19.8	279.5	259.9	1	4	20.0	36.40	34.30	38.40
1141	53.65	207.10	21.4	22.0	279.7	288.8	1	4	23.0	36.30	34.30	38.20
1141	53.82	207.92	21.5	19.8	278.8	268.3	1	4	15.0	40.40	39.10	41.70
1141	53.85	207.84	21.5	20.6	278.9	259.2	1	4	7.0	40.30	38.80	41.70
1141	53.89	207.75	21.4	22.6	279.1	289.3	1	4	18.0	40.20	38.80	41.50
1141	53.02	208.63	22.0	19.6	276.5	264.2	1	3	17.0	40.40	39.20	41.70
1141	53.05	208.55	22.0	20.6	276.7	254.4	1	3	6.0	40.30	38.90	41.70
1141	53.09	208.46	22.0	22.4	276.9	276.6	1	3	19.0	40.20	38.90	41.50
1141	53.41	208.27	21.9	19.4	277.6	268.2	1	3	16.0	40.40	39.20	41.70
1141	53.44	208.19	21.9	20.1	277.8	260.3	1	3	6.0	40.30	38.90	41.70
1141	53.49	208.11	21.9	22.1	278.0	289.6	1	3	19.0	40.20	38.90	41.50
1141	53.69	208.85	21.9	21.4	276.9	250.8	1	3	15.0	43.90	43.10	44.80
1141	53.74	208.76	21.8	23.8	277.1	290.3	1	3	27.0	43.80	43.10	44.50
1141	53.20	209.60	22.3	20.5	274.9	270.3	1	4	18.0	45.30	43.40	47.20
1141	53.29	209.20	22.2	20.7	275.8	250.9	1	4	16.0	43.90	43.10	44.70
1141	53.39	209.45	22.3	20.1	275.3	244.2	1	4	27.0	45.30	43.10	47.50
1141	53.33	209.11	22.2	22.3	276.0	273.8	1	4	29.0	43.80	43.10	44.50
1141	53.61	209.26	22.1	21.5	275.9	277.0	1	4	19.0	45.30	43.40	47.20
1141	53.80	209.10	21.9	21.0	276.5	245.9	1	4	27.0	45.30	43.10	47.50
1141	53.87	209.90	21.9	21.1	274.6	269.1	1	4	17.0	48.50	47.30	49.70
1141	53.07	210.58	22.3	21.4	272.6	273.1	1	3	18.0	48.50	47.30	49.70
1141	53.16	210.81	22.4	20.4	272.0	265.5	1	3	27.0	49.60	47.30	51.90
1141	53.24	210.43	22.4	19.6	273.0	237.2	1	3	10.0	48.50	47.00	50.00
1141	53.47	210.24	22.3	21.2	273.5	273.0	1	3	18.0	48.50	47.30	49.70
1141	53.57	210.48	22.3	20.6	272.9	268.6	1	3	27.0	49.60	47.30	52.00
1141	53.65	210.09	22.2	20.6	273.9	234.8	1	3	11.0	48.50	47.00	50.00
1141	53.98	210.15	21.8	21.2	274.0	270.2	1	3	30.0	49.60	47.30	52.00
1141	53.91	210.75	22.0	20.3	272.2	233.5	1	3	22.0	51.50	50.60	52.30
1141	53.04	211.76	22.4	19.7	269.4	266.3	1	3	7.0	52.50	51.00	54.00
1141	53.06	211.67	22.4	20.8	269.7	249.1	1	3	16.0	52.30	50.70	54.00
1141	53.09	211.40	22.4	19.7	270.4	233.5	1	3	25.0	51.50	50.70	52.20
1141	53.44	211.44	22.4	20.2	270.1	266.5	1	3	7.0	52.50	51.00	54.00
1141	53.39	211.55	22.4	17.9	269.8	246.9	1	3	23.0	52.70	51.00	54.30

TABLE 1b, Sample Data Listing from Rev. 1141, Right Side

11 THETA	12 FOR THETA	13 AFT THETA	14 FOR AZ	15 AFT AZ	16 NRCS, FOR	17 NRCS, AFT	18 NSD, FOR	19 NSD, AFT	20 POL, FOR	21 POL, AFT
34.60	34.40	34.80	18.91	109.34	-10.84	-6.66	6.5	5.5	0	1
34.50	34.40	34.60	18.91	109.57	-10.84	-8.41	6.5	5.6	0	0
36.50	34.60	38.40	19.13	109.57	-9.62	-8.32	6.5	4.4	1	1
36.40	34.30	38.40	18.65	109.57	-10.84	-8.32	6.5	4.4	0	1
36.30	34.30	38.20	18.65	109.76	-10.84	-10.18	6.5	4.5	0	0
40.40	39.10	41.70	19.65	110.05	-11.19	-9.27	4.9	3.6	1	1
40.30	38.80	41.70	19.21	110.05	-13.16	-9.27	5.0	3.6	0	1
40.20	38.80	41.50	19.21	110.21	-13.16	-11.83	5.0	3.8	0	0
40.40	39.20	41.70	20.16	110.47	-11.01	-9.54	4.9	3.6	1	1
40.30	38.90	41.70	19.73	110.47	-13.00	-9.54	5.0	3.6	0	1
40.20	38.90	41.50	19.73	110.66	-13.00	-12.17	5.0	3.8	0	0
40.40	39.20	41.70	19.92	110.27	-11.39	-9.47	4.9	3.6	1	1
40.30	38.90	41.70	19.48	110.27	-13.47	-9.47	5.0	3.6	0	1
40.20	38.90	41.50	19.48	110.44	-13.47	-11.94	5.0	3.8	0	0
43.90	43.10	44.80	20.04	110.74	-14.76	-10.38	3.8	3.2	0	1
43.80	43.10	44.50	20.04	110.89	-14.76	-12.94	3.8	3.5	0	0
45.30	43.40	47.20	20.68	111.75	-12.35	-16.07	3.6	4.1	1	0
43.90	43.10	44.70	20.28	110.96	-15.12	-10.71	3.9	3.2	0	1
45.30	43.10	47.50	20.28	111.42	-15.12	-12.15	3.9	3.4	0	1
43.80	43.10	44.50	20.28	111.11	-15.12	-13.81	3.9	3.6	0	0
45.30	43.40	47.20	20.45	111.55	-12.22	-15.35	3.7	3.9	1	0
45.30	43.10	47.50	20.04	111.22	-14.76	-11.61	3.8	3.3	0	1
48.50	47.30	49.70	21.00	112.00	-13.02	-16.98	3.1	5.0	1	0
48.50	47.30	49.70	21.44	112.39	-13.11	-16.71	3.1	4.9	1	0
49.60	47.30	51.90	21.44	112.82	-13.11	-18.37	3.1	6.7	1	0
48.50	47.00	50.00	21.06	112.08	-17.02	-13.44	3.7	4.0	0	1
48.50	47.30	49.70	21.23	112.19	-13.23	-16.84	3.1	5.0	1	0
49.60	47.30	52.00	21.23	112.63	-13.23	-18.21	3.1	6.6	1	0
48.50	47.00	50.00	20.83	111.89	-16.40	-13.11	3.6	4.0	0	1
49.60	47.30	52.00	21.00	112.44	-13.02	-17.84	3.1	6.4	1	0
51.50	50.60	52.30	21.40	112.36	-18.01	-13.75	4.6	5.0	0	1
52.50	51.00	54.00	22.19	113.42	-14.21	-19.49	3.7	8.5	1	0
52.30	50.70	54.00	21.82	113.42	-18.36	-19.49	4.7	8.5	0	0

THEORETICAL CONSIDERATIONS

The objectives of this analysis of the SASS data are to recover the synoptic scale wind at a one degree resolution on a spherical coordinate grid and to derive synoptic scale fields for divergence, vertical velocity, the vector wind stress, and the curl of the winds stress from these winds. For use in a synoptic scales analysis at some initial time, the requirement is for the winds to be specified as east-west and north-south components at integral intersections of latitude and longitude in the form of values as close as possible to $U_s(\lambda_o,\theta_o)$ and $V_s(\lambda_o,\theta_o)$, where the subscript, s, designates an error free synoptic scale measurement with synoptic scale gradients accounted for and their effects removed and with mesoscale fluctuations and instrument errors reduced.* The SASS winds were not measured at the location, λ_o,θ_o. They contain the effects of mesoscale variability, and there are errors (sampling variability as an effect of communication noise and cell location inaccuracies), in the measurement of the backscatter that in turn result in errors in the calculated winds.

The locations of the SASS measurements are more or less randomly distributed in an area around the desired location, λ_o,θ_o, but the gradients in the wind are systematic and need to be considered. If the SASS-1 wind vector recovery algorithm and model function have no systematic bias, the mesoscale fluctuations and the effects of communication noise will also be random and have the same probabilistics and statistical properties within an area around λ_o,θ_o.

The individual SASS winds can be combined in such as way that the effects of gradients can be greatly reduced as a source of error in finding the wind at λ_o,θ_o. Also the random errors introduced by mesoscale variability and communication noise, can be modeled probabilistically, interpreted statistically and greatly reduced by means of the application of small sample theory.

It is not necessary to separate the combined effects of mesoscale variability and communication noise. Their effects can, however, be considered in

---

*An appendix defines the notation

the interpretation of the results that are obtained. Often the effects of communication noise stand out above the effects of mesoscale variability especially as a function of aspect angle relative to the pointing angles of the radar beams of the SASS.

Consider a number of measurements, all of the same geophysical quantity such as some kind of a wind represented by u, made in the same area, that all ought to be nearly equal to the same value. These values will not be equal for numerous reasons. Conceptually there is some correct (or true) value and the actual values will scatter in a random way about this correct value. The measurements can be described as having a probability density function (pdf), $f(u)$, with the usual properties of a pdf, namely,

$$f(u) \geq 0 \tag{1}$$

$$\int_{-\infty}^{\infty} f(u)\, du = 1 \tag{2}$$

and $$\int_{-\infty}^{\infty} u f(u)\, du = u_1 \tag{3}$$

which is the first moment of the pdf and can be associated with the correct value.

Moments about u_1 as in

$$u' = u - u_1$$

yield $$\int_{-\infty}^{\infty} (u - u_1)\, f(u)\, du = 0 \tag{4}$$

and $$\int_{-\infty}^{\infty} (u - u_1)^2\, f(u)\, du = (\Delta u)^2 \tag{5}$$

Now let $$u = u_1 + t\Delta u \tag{6}$$

or $$t = (u - u_1)/\Delta u \tag{7}$$

so that $f(u)$ is transformed into $f(t)$. The pdf, $f(u)$, is transformed into

$$f(u_1 + t\Delta u)\Delta u\, dt = f^*(t)\, dt \tag{8}$$

and $f^*(t)dt$ has the properties that

$$\int_{-\infty}^{\infty} f^*(t)dt = 1 \tag{9}$$

$$\int_{-\infty}^{\infty} t\, f^*(t)dt = 0 \tag{10}$$

$$\int_{-\infty}^{\infty} t^2\, f^*(t)dt = 1 \tag{11}$$

The concept can be generalized if various reasons for the variability of the measurements can be identified. Suppose that there are, say, two causes for the variability that many differ from one set of measurements to another such that

$$(\Delta u)^2 = (\Delta u_1)^2 + (\Delta u_2)^2 \tag{12}$$

Then the pdf can be generalized to the product of two independent pdf's, $f(t_1) \cdot f(t_2)$, and (7) becomes

$$u = u_1 + t_1\, \Delta u_1 + t_2\, \Delta u_2 \tag{13}$$

with obvious extentions, if needed, such as, for example, conditions such that t_1 and t_2 are not independent and covariances are needed.

Small sample theory can be applied under the assumption that all of the measurements are for the purpose of learning more about u_1. Suppose that M measurements are made as in

$$u_i = u_1 + t_{1i}\, \Delta u_1 + t_{2i}\, \Delta u_2 \tag{14}$$

where the t_{1i} and t_{2i} are from (not necessarily the same) pdf's with properties defined by (10), (11) and (12). ($f^*(t)$ is the convolution of $f(t_1)$ and $f(t_2)$).

The average value of the u_i is given by (16) from (11)

$$\bar{u} = \frac{1}{M}\sum_{1}^{M} u_i$$

$$= u_1 + \frac{1}{M}\sum t_{1i}\,\Delta u_1 + \frac{1}{M}\sum t_{2i}\,\Delta u_2$$

$$= u_1 + \frac{1}{M}\sum t_i\,\Delta u = u_1 + \frac{1}{M}\sum t\left[(\Delta u_1)^2 + (\Delta u_2)^2\right]^{1/2} \tag{15}$$

and the expected value of the average is (16).

$$\mathcal{E}(\bar{u}) = u_1 \tag{16}$$

The random variable

$$t_1^* = \frac{1}{M}\sum t_{1i} \tag{17}$$

has a mean of zero and a second moment of

$$M_2(t_1^*) = 1/M \tag{18}$$

so that $\bar{u}$ can be represented by

$$\bar{u} = u_1 + t_1^*(M^{-1/2}\,\Delta u_1) + t_2^*(M^{-1/2}\,\Delta u_2)$$

$$= u_1 + t^*\left[M^{-1}((\Delta u_1)^2 + (\Delta u_2)^2)\right]^{1/2} \tag{19}$$

The expected value of $\bar{u}$ is u_1 and the expected value of $(\bar{u}-u_1)^2$ is

$$\mathcal{E}(\bar{u} - u_1)^2 = M^{-1}\left[(\Delta u_1)^2 + (\Delta u_2)^2\right] \tag{20}$$

From a given sample, it is possible to estimate the mean, $\bar{u}$, the standard deviation, Δu, and to use the fact that $\bar{u}$ has a standard deviation with reference to the desired true value given by $M^{-1/2}\,\Delta u$ where M is the sample size.

A number of SASS individual wind values can be combined in such a way as to recover a single estimate with a greatly reduced variability. When these estimates are then combined to form fields, this greatly reduced variability, which is known, can be used to find the variability of various derived fields.

It is well known that the mean of a sample from almost any typical, but unknown, pdf will be nearly normally distributed by virtue of the central limit theorem so that although the pdf's of t, t_1, and t_2 may not be known, the pdf's of t^*, t_1^* and t_2^* will be close to a unit variance zero mean normal pdf for most of the values of M that occur in what follows.

As in any statistical proceedure the moments of a pdf, such as u_1, always remain unknown. The statistics only provide a way to put bounds on the estimate of u_1, that is $\bar{u}$, that are made narrower because of the sample size. In (15), $\bar{u}$, M, $(\Delta u_1)^2 + (\Delta u_2)^2 = (\Delta u)^2$ are all known statistics, where $(\Delta u_1)^2 + (\Delta u_2)^2$ is an estimate of the variance from the sample. Thus (15) can be rewritten as

$$u_1 = \bar{u} - t^* M^{-\frac{1}{2}} \Delta u \qquad (21)$$

where all is known on the RHS except t^* (the minus sign is not too relevant). The values of u_1 when found at a grid of points form a field consisting of values of $\bar{u}$ plus a quantity that provides information on the variability of $\bar{u}$.

As an example, if $\bar{u}$ is 10.73 m/s, Δu is 2 m/s, and M is 25, then about two thirds of the time it would be expected that the interval 10.33 to 11.13 m/s would enclose the true value, u_1. If sampling variability quantities are kept track of in the finite difference calculations of properties of the wind field, they provide estimates of the sampling variability of these properties.

PRELIMINARY DATA PROCESSING

The first data processing step was to sort the data shown as an example in Table 1 for each revolution into overlapping two degree by two degree sets centered on the one degree integer values of latitude and longitude. The vector winds found from combining many individual SASS winds around a grid point of a model have been called superobservations. A given SASS wind could be found in four different sets. As in Figure 1, a given set of SASS winds would have latitudes and longitudes that varied from $\lambda_o - 1$ to $\lambda_o + 1$ and $\theta_o - 1$ to $\theta_o + 1$.

A preliminary investigation suggested that the two solution cases and the base of the "Y" in three solution cases gave both directions and speeds that were systematically different from the other directions and speeds within a given two degree square. Since the original data set gives the pointing direction of beam 1, say, χ_o, dealiased winds were checked to see if the directions were within $\chi_o \pm 1^o$, χ_o plus 89^o to 91^o, χ_o plus 179^o to 181^o, and χ_o plus 269^o to 271^o. If they were, those particular data vectors were removed from the set. In Table 1a, for example, the data corresponding to SASS directions of 288.8, 289.3, 289.6 and 290.3, were deleted.

When centered on λ_o and θ_o, the latitudes and longitudes can be transformed by subtracting λ_o and θ_o from each element in the set. The locations of each SASS wind will then be defined by values of, $\Delta\lambda$ and $\Delta\theta$ that both range between plus and minus one.

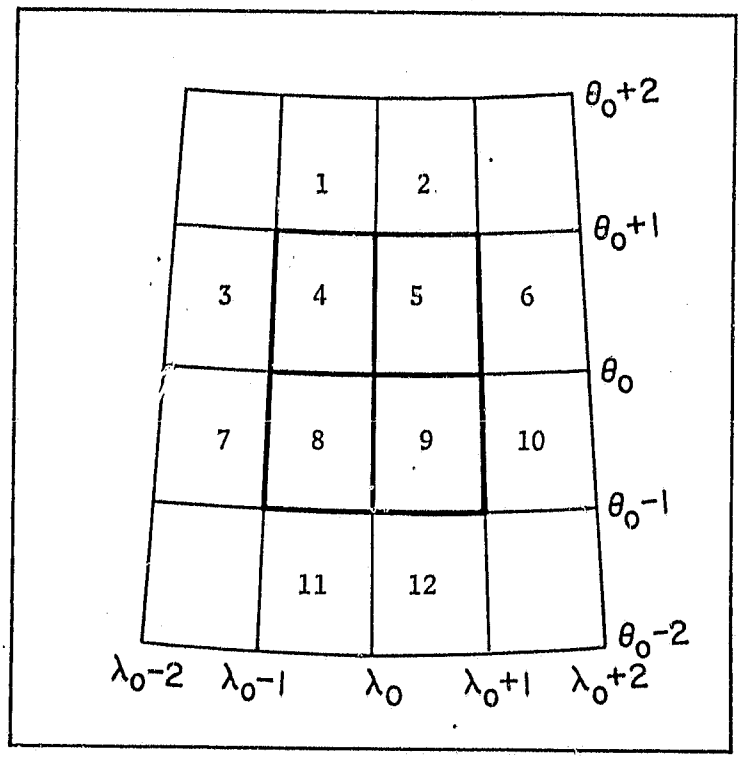

Fig. 1 The 2° by 2° Overlapping Spherical Coordinate Grid Centered on Integer Values of Latitude and Longitude.

The average latitude and longitude for the data set will be equations (22) and (23) for the N + n values in the 2 degree square.

$$\lambda_o + \overline{\Delta\lambda}_1 = \lambda_o + \frac{1}{N+n}\sum_{1}^{N+n}\Delta\lambda_j \tag{22}$$

$$\theta_o + \overline{\Delta\theta}_1 = \theta_o + \frac{1}{N+n}\sum_{1}^{N+n}\Delta\theta_j \tag{23}$$

The values of $\overline{\Delta\lambda}$ and $\overline{\Delta\theta}$ will usually be close to, but not exactly, zero. The location of this point will be in one of the four quadrants of the heavy square in Figure 1. By selectively removing n of the data vectors in the set based on the location of $\overline{\Delta\lambda}$ and $\overline{\Delta\theta}$, it is possible to reduce both $\overline{\Delta\lambda}$ and $\overline{\Delta\theta}$ for the remaining subset below some preassigned minimum as in equations (24) and (25).

$$\lambda_o + \overline{\Delta\lambda} = \lambda_o + \frac{1}{N}\sum_{1}^{N}\Delta\lambda_i \tag{24}$$

$$\theta_o + \overline{\Delta\theta} = \theta_o + \frac{1}{N}\sum_{1}^{N}\Delta\theta_i \tag{25}$$

This subset of data for each two by two degree square was processed further to obtain the results to follow. Also needed for later use will be the average values of $(\Delta\lambda_i)^2$, $(\Delta\theta_i)^2$ and $(\Delta\lambda_i \cdot \Delta\theta_i)$.

WIND VECTORS

The N value for the winds in each data set consisted of a speed and a (from which) direction (meteorological convention, clockwise from north). The directions were averaged to obtain a value for the average direction as in (26) where the summation notation is abbreviated.

$$\bar{\chi} = \frac{1}{N}\sum \chi_i \tag{26}$$

Each wind was then resolved into a component in the direction of $\bar{\chi}$ and a component normal to $\bar{\chi}$ as in (27) and (28).

$$V_{Pi} = |V|_i \cos(\chi_i - \bar{\chi}) \tag{27}$$

$$V_{Ni} = |V|_i \sin (\chi_i - \bar{\chi}) \tag{28}$$

These components were averaged to obtain (29) and (30).

$$\bar{V}_P = \frac{1}{N} \sum V_{Pi} \tag{29}$$

$$\bar{V}_N = \frac{1}{N} \sum V_{Ni} \cong 0 \tag{30}$$

In all cases $\bar{V}_N$ was essentially zero. The standard deviations of $\bar{V}_P$ and $\bar{V}_N$ about their sample means were also computed as in (31) and (32).

$$\Delta u = SD(V_P) = \left(\frac{1}{N} \sum (V_{Pi} - \bar{V}_P)^2\right)^{\frac{1}{2}} \tag{31}$$

$$\Delta v = SD(\bar{V}_N) = \left(\frac{1}{N} \sum V_{Ni} - \bar{V}_N)^2\right)^{\frac{1}{2}} \tag{32}$$

The processed data at this point consist of the sample size, N, the mean direction, $\bar{\chi}$, the mean component in the mean direction, $\bar{V}_P$ and the values of ΔU and ΔV as located at a point given by $\lambda_o + \overline{\Delta\lambda}$ (with the values of $\lambda_o + \overline{\Delta\lambda}$ and $\theta_o + \overline{\Delta\theta}$ located very close to the integer values of latitude and longitude over the ocean) plus the average values of $(\Delta\lambda_j)^2$, $(\Delta\theta_j)^2$ and $\Delta\lambda_j \, \Delta\theta_j$ (i.e. VAR ($\Delta\lambda$), VAR ($\Delta\theta$) and COV ($\Delta\lambda\Delta\theta$).

The "from which" meteorological convention can be converted t a "toward which" vector by adding 180^o (mod 360^o). The new direction, clock angle, is needed for use in analyzing the wind field. The east-west, U_λ, (abbreviated as U), and the north-south, V_θ, (abbreviated as V) components of the three non-zero vectors given by (29), (31), and (32) are next found.

The mean east-west and north-south components are given by (33) and (34).

$$\bar{U} = \bar{V}_P \sin (\bar{\chi} + 180^o) = -\bar{V}_P \sin \bar{\chi} \tag{33}$$

$$\bar{V} = \bar{V}_P \cos (\bar{\chi} + 180^o) = -\bar{V}_P \cos \bar{\chi} \tag{34}$$

The components of ΔU and ΔV from (31) and (32) in the east-west direction according to the convention shown in Figure 2 are (35) and (36).

$$\Delta u_1 = -\Delta u \sin \bar{\chi} \tag{35}$$

$$\Delta u_2 = -\Delta v \cos \bar{\chi} \tag{36}$$

The components in the north-south direction are given by (37) and (38).

$$\Delta v_1 = -\Delta u \cos \bar{\chi} \tag{37}$$

$$\Delta v_2 = \Delta v \sin \bar{\chi} \tag{38}$$

The vectors $(V_p, \bar{\chi})$, $(\Delta U, \bar{\chi})$ and $(\Delta V, \bar{\chi} + 90^o)$, can be used to form two orthogonal vectors, as in (39) and (40).

$$V_{Ps} = \bar{V}_P - t_1 \Delta u \tag{39}$$

$$V_{Ns} = \bar{V}_N - t_2 \Delta v = 0 - t_2 \Delta v \tag{40}$$

and $\bar{\chi} = \chi_s$. The subscript, s, represents the desired synoptic scale value.

The orthogonal coordinate system has one axis parallel to the direction, $\bar{\chi}$, and t_i and t_2 are independent random variables with zero means and unit standard deviations as in equation (9) to (11). When resolved into north-south and east-west components, east-west variability is correlated with north-south variability so as to confine the scatter of points to the form of ellipses such as the one shown by the dashed line in Figure 2. The variability of $\bar{U}$ and $\bar{V}$, where U_s and V_s are the desired synoptic scale components, analogous to u_1 in equation (7), can be represented by (41) and (42). The calculated values, $\bar{U}$ and $\bar{V}$, equal the true values U_s and V_s, plus the effects of gradients and the random errors.

$$\bar{U}(\lambda_o + \overline{\Delta\lambda}, \theta_o + \overline{\Delta\theta}) = U_s(\lambda_o + \overline{\Delta\lambda}, \theta_o + \overline{\Delta\theta}) + t_1 \Delta u_1 + t_2 \Delta u_2 \tag{41}$$

$$\bar{V}(\lambda_o + \overline{\Delta\lambda}, \theta_o + \overline{\Delta\theta}) = V_s(\lambda_o + \overline{\Delta\lambda}, \theta_o + \overline{\Delta\theta}) + t_1 \Delta v_1 + t_2 \Delta v_2 \tag{42}$$

Following these transformations, the data for each integer value of latitude and longitude for each point in the SASS swath consists of λ_o,

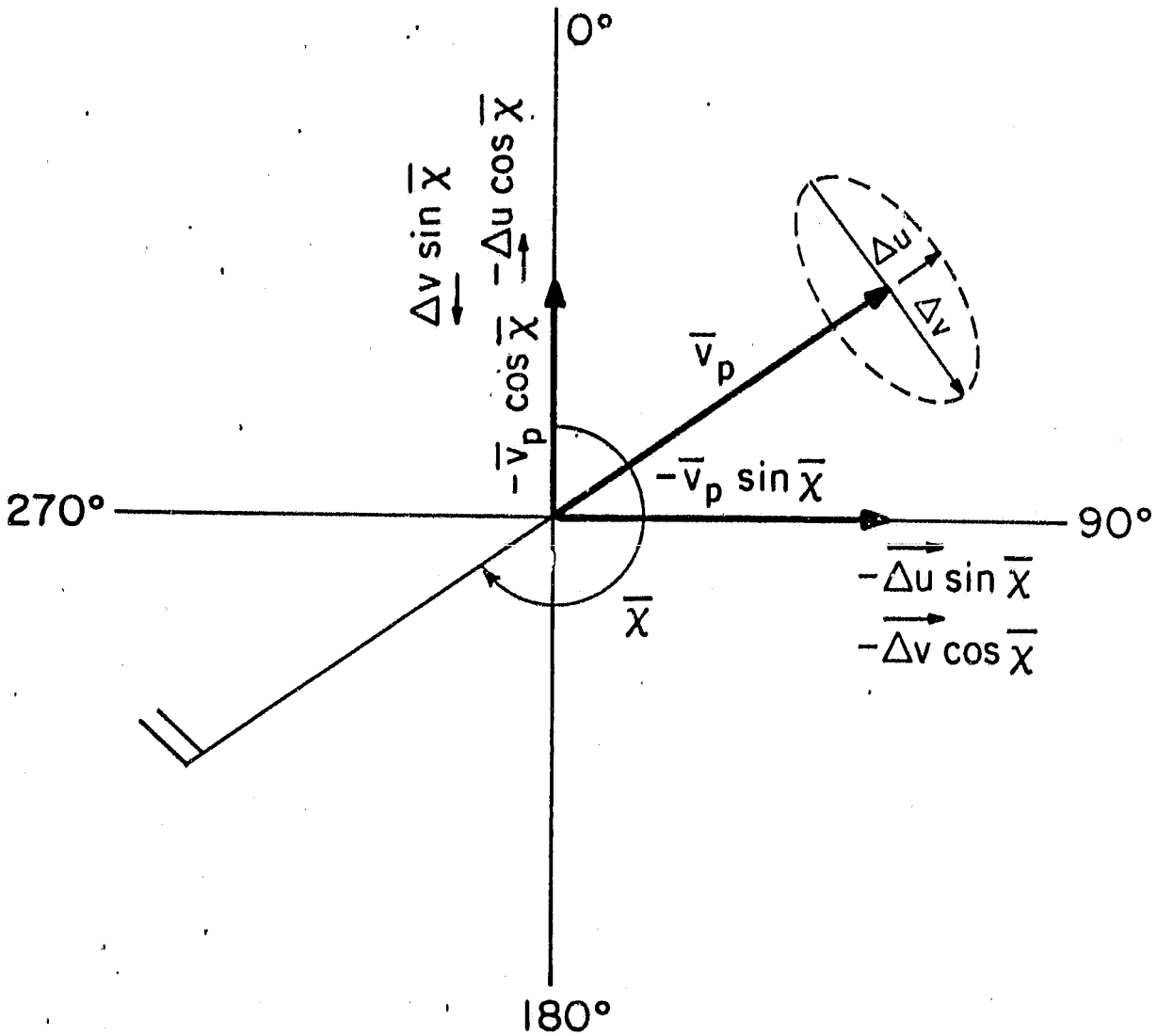

Fig. 2 Conventions for the Conversion of $\bar{v}_p$, $\bar{\chi}$, Δu, and Δv to $\bar{u}, \bar{v}, \Delta u_1, \Delta u_2, \Delta v_1$ and Δv_2.

θ_o, $\overline{\Delta\lambda}$, $\overline{\Delta\theta}$, $\bar{U}$, ΔU_1, ΔU_2, $\bar{V}$, ΔV_1, ΔV_2, VAR($\Delta\lambda$), VAR($\Delta\theta$), COV($\Delta\lambda\Delta\theta$) and N. The following steps process the $\bar{U}$ and $\bar{V}$ components of the processed SASS data to determine the best possible field for the synoptic scale wind.

Consider the east-west component of the wind at a point where it was estimated by the SASS somewhere within the two degree square. The value could be described by equation (43).

$$U(\lambda_i, \theta_i) = U_s(\lambda_o, \theta_o) + \frac{\partial U_s(\lambda_o, \theta_o)}{\partial \lambda}(\lambda_i - \lambda_o) + \frac{\partial U_s(\lambda_o, \theta_o)}{\partial \theta}(\theta_i - \theta_o) + t_i \Delta U' \quad (43)$$

where $\Delta U'$ is to be defined later.

The average value of the N values of $U(\lambda_i, \theta_i)$ is

$$\bar{U} = \frac{1}{N}\sum (U(\lambda_i, \theta_i)) = \bar{U}(\lambda_o + \overline{\Delta\lambda}, \theta_o + \overline{\Delta\theta})$$

$$= U_s(\lambda_o, \theta_o) + \frac{\partial U_s(\lambda_o, \theta_o)}{\partial \lambda}\overline{\Delta\lambda} + \frac{\partial U_s(\lambda_o, \theta_o)}{\partial \theta}\overline{\Delta\theta} + \frac{1}{N}\sum t_i \Delta U' \quad (44)$$

Everything except $U_s(\lambda_o, \theta_o)$ is known, or can be estimated, and the two other terms on the right hand side are usually small because $\overline{\Delta\lambda}$ and $\overline{\Delta\theta}$ are small. For points in the interior of the swath, it is possible to estimate a correction from the gradients of $\bar{U}$ as in (45) where uncorrected values near the grid points are used to find approximate gradients,

$$\bar{U}(\lambda_o, \theta_o) = \bar{U}(\lambda_o + \overline{\Delta\lambda}, \theta_o + \overline{\Delta\theta}) - \tfrac{1}{2}(\bar{U}(\lambda_o + 1 + \overline{\Delta\lambda}, \theta_o + \overline{\Delta\theta}) - \bar{U}(\lambda_o - 1 + \overline{\Delta\lambda}, \theta_o + \overline{\Delta\theta}))\overline{\Delta\lambda} - \tfrac{1}{2}(\bar{U}(\lambda_o + \overline{\Delta\lambda}, \theta_o + 1 + \overline{\Delta\theta}) - \bar{U}(\lambda_o - 1\,\overline{\Delta\lambda}, \theta_o - 1 + \overline{\Delta\theta}))\overline{\Delta\theta} \quad (45)$$

subject to the conditions that appropriate inequalities hold, namely

either $\bar{U}(\lambda_o + 1 + \overline{\Delta\lambda}, \theta_o + \overline{\Delta\theta}) > \bar{U}(\lambda_o + \overline{\Delta\lambda}, \theta_o + \overline{\Delta\theta}) > \bar{U}(\lambda_o - 1 + \overline{\Delta\lambda}, \theta_o + \overline{\Delta\theta})$ (46)

or $\bar{U}(\lambda_o + 1 + \overline{\Delta\lambda}, \theta_o + \overline{\Delta\theta}) < \bar{U}(\lambda_o + \overline{\Delta\lambda}, \theta_o + \overline{\Delta\theta}) < \bar{U}(\lambda_o - 1 + \overline{\Delta\lambda}, \theta_o + \overline{\Delta\theta})$ (47)

and either $\bar{U}(\lambda_o + \overline{\Delta\lambda}, \theta_o + 1 + \overline{\Delta\theta}) > \bar{U}(\lambda_o + \overline{\Delta\lambda}, \theta_o + \overline{\Delta\theta}) > \bar{U}(\lambda_o + \overline{\Delta\lambda}, \theta_o - 1 + \overline{\Delta\theta})$ (48)

or $\bar{U}(\lambda_o + \overline{\Delta\lambda}, \theta_o + 1 + \overline{\Delta\theta}) < \bar{U}(\lambda_o + \overline{\Delta\lambda}, \theta_o + \overline{\Delta\theta}) < \bar{U}(\lambda_o + \overline{\Delta\lambda}, \theta_o - 1 + \overline{\Delta\theta})$ (49)

If sets of these inequalities are not satisfied, then $U(\lambda_o, \theta_o)$ is near a maximum or a minimum, in one or both directions, (or a saddle point) and the correction is simply to set $U(\lambda_o, \theta_o)$ equal to $U(\lambda_o + \overline{\Delta\lambda}, \theta_o + \overline{\Delta\theta})$.

The expected value of the square of $U(\lambda_i, \theta_i) - \bar{U}(\lambda_o, \theta_o)$ is given from (43) by (50).

$$\mathcal{E}\left(\frac{1}{N}\sum (U(\lambda_i,\theta_i) - \bar{U}(\lambda_o,\theta_o))^2\right.$$
$$= \left(\frac{\partial U_s(\lambda_o,\theta_o)}{\partial\lambda}\right)^2 \mathrm{VAR}(\Delta\lambda) + \left(\frac{\partial U_s(\lambda_o,\theta_o)}{\partial\theta}\right)^2 \mathrm{VAR}(\lambda\theta)$$
$$+ 2\,\frac{\partial U_s(\lambda_o,\theta_o)}{\partial\lambda}\,\frac{\partial U_s(\lambda_o,\theta_o)}{\partial\theta}\,\mathrm{COV}(\Delta\lambda\,\Delta\theta) + (\Delta U')^2 \qquad (50)$$

In (50), the first three terms represent the effects of gradients of the east-west component of the wind. These and similar terms contribute to the variability of U and V in (31) and (32) and of ΔU_1, ΔU_2, ΔV_1 and ΔV_2 in (41) and (42). These effects need to be removed so that the effects of sampling variability can be found.

The contribution of the variability of the values of $U(\lambda_i, \theta_i)$ and $V(\lambda_i, \theta_i)$ from gradients in the synoptic scale wind is the first three terms in (45). For SASS values uniformly scattered over a particular two degree by two degree square, the average values of $(\Delta\lambda_i)^2$ and $(\Delta\theta_i)^2$ will be about one third and the average value of $\Delta\lambda_i, \Delta\theta_i$ will be close to zero. SASS winds concentrated in diagonally opposed quadrants would yield a non-zero value for this third term. The synoptic scale contribution to the variability of the estimate of $U_s(\lambda_o, \theta_o)$ can be estimated by (51) where the values corrected by (45) have been used.

$$\mathrm{VAR}(\mathrm{SYNOPTIC}) = \frac{1}{4}(\bar{U}(\lambda_o + 1, \theta) - \bar{U}(\lambda_o - 1, \theta))^2\,\mathrm{VAR}\,\Delta\lambda$$
$$+ \frac{1}{4}(\bar{U}(\lambda_o, \theta_o + 1) - \bar{U}(\lambda_o, \theta_o - 1))^2\,\mathrm{VAR}\,\Delta\theta$$
$$+ \frac{1}{2}(\bar{U}(\lambda_o + 1, \theta_o) - \bar{U}(\lambda_o - 1, \theta_o))(\bar{U}(\lambda_o, \theta_o + 1) - \bar{U}(\lambda_o, \theta_o - 1))\,\mathrm{COV}\,\Delta\lambda\Delta\theta \qquad (51)$$

The variability of the estimate, $\bar{U}(\lambda_o,\theta_o)$, that is the result of mesoscale variability of the winds from one SASS cell to the other and of the effects of communication noise is found by means of (52).

$$\text{VAR (MESO PLUS COMMUNICATION NOISE)} = (\Delta U_1)^2 + (\Delta U_2)^2 - \text{VAR (SYNOPTIC)}$$

$$= (\Delta U')^2 \qquad (52)$$

where $(\Delta U')$ is now defined in (43) by equation (52). Since VAR(SYNOPTIC) is an estimate, it may exceed $(\Delta U_1)^2 + (\Delta U_2)^2$ in which case $(\Delta U')^2$ is set to zero. The analyses of superobservations by Pierson (1982, 1983) assumed that gradients of the synoptic scale wind could be neglected in the study of superobservations. For some parts of the wind fields obtained from the SASS, the assumption is not justified, and this correction needs to be made. Often it is small. Specific examples will be given later.

A parallel set of equations for the north-south components of the synoptic scale winds can also be obtained. The final results of processing the data in this way produces values of $\bar{U}(\lambda_o,\theta_o)$, $\bar{V}(\lambda_o,\theta_o)$, $\Delta U'$ and $\Delta V'$ at the integer values of λ and θ in the main part of the SASS swath where $\overline{\Delta\lambda}$ are $\overline{\Delta\theta}$ small. Near the edges of the SASS swath, which will be discussed separately, other methods are needed because of the smaller number of values in the superobservation, the location of the data fairly far from the desired latitude and longitude and the lack of values for all of the quantities needed in the above equations.

The elliptical scatter of the winds that form a superobservation is an important aspect of the sampling variability of the measurements. From (52), and its equivalent for V and from (35), (36), (37) and (38), reduced values of ΔU_1 and ΔU_2 may prove useful in studying the effects of mesoscale variability and communication noise.

Let

$$K = \left[(\Delta U')^2 + (\Delta V')^2\right] \left[(\Delta U_1)^2 + (\Delta U_2)^2 + (\Delta V_1)^2 + (\Delta V_2)^2\right]^{-1} \qquad (53)$$

Then let

$$\Delta U_1' = K^{\frac{1}{2}} \Delta U_1 \tag{54}$$

$$\Delta U_2' = K^{\frac{1}{2}} \Delta U_2 \tag{55}$$

$$\Delta V_1' = K^{\frac{1}{2}} \Delta V_1 \tag{56}$$

$$\Delta V_2' = K^{\frac{1}{2}} \Delta V_2 \tag{57}$$

This change effectively reduces the elliptical scatter of the original data by an amount attributable to the removal of synoptic scale variability over the two degree by two degree square.

The final result of the steps taken so far is to make it possible to represent the east-west and north-south components of the synoptic scale wind at λ_o, θ_o in forms similar to equations (19) and (21). They are equations (58) and (59) and equations (60) and (61).

$$\bar{U}(\lambda_o, \theta_o) = U_s(\lambda_o, \theta_o) + t_1 N^{-\frac{1}{2}} \Delta U_1' + t_2 N^{-\frac{1}{2}} \Delta U_2' \tag{58}$$

$$\bar{V}(\lambda_o, \theta_o) = V_s(\lambda_o, \theta_o) + t_1 N^{-\frac{1}{2}} \Delta V_1' + t_2 N^{-\frac{1}{2}} \Delta V_2' \tag{59}$$

$$U_s(\lambda_o, \theta_o) = \bar{U}(\lambda_o, \theta_o) - t_1 N^{-\frac{1}{2}} \Delta U_1' - t_2 N^{-\frac{1}{2}} \Delta U_2' \tag{60}$$

$$V_s(\lambda_o, \theta_o) = \bar{V}(\lambda_o, \theta_o) - t_1 N^{-\frac{1}{2}} \Delta V_1' - t_2 N^{-\frac{1}{2}} \Delta V_2' \tag{61}$$

For an analysis of (58) and (59), the same values for t_1 and t_2 must be used in both equations. This shows that $\bar{U}$ and $\bar{V}$ are not independent and for example that

$$\mathcal{E}\left\{\left[\left(\bar{U}(\lambda_o, \theta_o) - U_s(\lambda_o, \theta_o)\right)\left(\bar{V}(\lambda_o, \theta_o) - V_s(\lambda_o, \theta_o)\right)\right]\right\} \tag{62}$$

$$= N^{-1}\left(\Delta U_1' \Delta V_1' + \Delta U_2' \Delta V_2'\right) \tag{63}$$

Equations (60) and (61) put all of the known statistics on the right hand side. It needs to be interpreted with care. There is, conceptually, only one correct value for U_s, and only one, for V_s. Picking t_1 and t_2 at random generates many values of U_s and V_s, one of which may be the correct one. It t_1 and t_2 are constrained to lie on a circle and are normally

distributed then

$$P(t_1^2 + t_2^2 < R^2) = \frac{1}{2\pi} \iint_{t_1^2 + t_2^2 = R^2} e^{-(t_1^2 + t_2^2)/2} \, dt_1 \, dt_2$$

$$= \frac{1}{2\pi} \int_0^R \int_0^{2\pi} e^{-\zeta^2/2} \zeta \, d\zeta \, d\theta$$

$$= 1 - e^{-R^2/2}$$

so that if $R = 2$, the ellipse generated in the U_s V_s plane will have a probability of 0.865 of enclosing the true value of U_s and V_s.

In the analysis of superobservations, each SASS wind in the four degree square is given equal weight in contrast to some of the present analysis techniques that weight wind and pressure reports from ships as a function of how far away they are from the grid point being analysed. For conventional data and conventional analysis procedures, the same report will influence a grid point from distances as far away as five or ten degrees of latitude or longitude. Other sources of error dominate the analysis of conventional data and maximum use must be made of each oceanic observation because of the poor spacing and sparceness of the data.

For SASS data the error sources are different and the dominant ones are essentially random. Equally weighted observations are the most effective way to reduce the variability inherent in the SASS data.

THE FIELD OF HORIZONTAL DIVERGENCE

For constant density at a fixed height above the sea surface, the equation of continuity in spherical coordinates is given by equation (64).

$$\frac{1}{R^2}\left(\frac{\partial}{\partial R}(R^2 W)\right) + \frac{1}{R\cos\theta}\frac{\partial U}{\partial \lambda} + \frac{1}{R\cos\theta}\frac{\partial(\cos\theta V)}{\partial\theta\,\partial\theta} = 0 \tag{64}$$

The divergence of the horizontal wind at 19.5 meters for a neutral atmosphere is given by equation (65).

$$\mathrm{div}_2 \mathbb{W}_h = \frac{1}{R\cos\theta}\left(\frac{\partial U}{\partial\lambda} + \cos\theta\frac{\partial V}{\partial\theta} - \sin\theta V\right) \tag{65}$$

A finite difference estimate of the divergence at a one degree resolution requires values of U at $\lambda_o + 1$, θ_o and $\lambda_o - 1$, θ_o and values of V at $\lambda_o, \theta + 1$; λ_o, θ_o and λ_o, $\theta_o - 1$. We neglect also the ellipticity of the Earth, and use $R = 2\cdot 10^7(\pi)^{-1}$. The equations are in the form of (60) and (61).

The finite difference value for the horizontal divergence of the wind is given by equation (66) where the various ΔU_1, and so on, are associated with the appropriate latitude and longitude.

$$\begin{aligned}\left(\mathrm{div}_2 \mathbb{W}_h\right)_s = \frac{4\cdot5\cdot10^{-6}}{\cos\theta_o}\Big[&\Big(\bar{U}(\lambda_o+1,\theta_o) - t_1\,\Delta U_1' - t_2\,\Delta U_2' - \bar{U}(\lambda_o-1,\theta_o) \\ &+ t_3\,U_1' + t_4\,\Delta U_2'\Big) + \cos\theta_o\Big(\bar{V}(\lambda_o,\theta_o+1) - t_5\,\Delta V_1' - t_6\,\Delta V_2' \\ &- \bar{V}(\lambda_o,\theta_o-1) + t_7\,\Delta V_1' + t_8\,\Delta V_2'\Big) - 0.0349065\sin\theta(\bar{V}(\lambda_o,\theta_o) \\ &- t_9\,\Delta V_1' - t_{10}\,\Delta V_2')\Big]\end{aligned} \tag{66}$$

The expected value of $(\mathrm{div}_2 \mathbb{W}_h)_s$ simplifies to equation (67).

$$\begin{aligned}\mathcal{E}\,(\mathrm{div}_2 \mathbb{W}_h)_s = \frac{4\cdot5\cdot10^{-6}}{\cos\theta_o}\Big(&\bar{U}(\lambda_o+1,\theta_o) - \bar{U}(\lambda_o-1,\theta_o) \\ &+ \cos\theta_o(\bar{V}(\lambda_o,\theta_o+1) - \bar{V}(\lambda_o,\theta_o-1)) \\ &- 0.0349065\,(\sin\theta_o\,\bar{V}(\lambda_o,\theta_o))\Big) = \overline{\mathrm{div}_2 \mathbb{W}_h}\end{aligned} \tag{67}$$

The expected value of the variance of the divergence is given by equation (68)

$$
\begin{aligned}
E\left[(\mathrm{div}_2 W_h)_s - (\overline{\mathrm{div}_2 W_h})\right]^2 &= \mathrm{VAR}\,(\mathrm{div}_2 W_h) \\
&= \frac{2.025\cdot 10^{-11}}{(\cos\theta_o)^2}\Big[\,(\Delta U_1'(\lambda_o+1,\theta_o))^2 + (\Delta U_2'(\lambda_o+1,\theta_o))^2 + (\Delta U_1'(\lambda_o-1,\theta_o))^2 \\
&\quad + (\Delta U_2'(\lambda_o-1,\theta_o))^2 + (\cos\theta_o)^2\,((\Delta V_1'(\lambda_o,\theta_o+1))^2 + (\Delta V_2'(\lambda_o,\theta_o+1))^2 \\
&\quad + (\Delta V_1'(\lambda_o,\theta_o-1))^2 + (\Delta V_2'(\lambda_o,\theta_o-1))^2) \\
&\quad + 1.2184\cdot 10^{-3}\,(\sin\theta_o)^2\,((\Delta V_1'(\lambda_o,\theta_o))^2 + (\Delta V_2'(\lambda_o,\theta_o))^2)\,\Big] \qquad (68)
\end{aligned}
$$

The divergence at one of the grid points in the SASS swath where sufficient data are available is thus given by equation (69) where t by the central limit theorem is approximately a normally distributed random variable with a zero mean and a unit variance.

$$(\mathrm{div}_2 W_h)_s = \overline{\mathrm{div}_2 W_h} + t\,(\mathrm{VAR}(\overline{\mathrm{div}_2 W_h}))^{\frac{1}{2}} \qquad (69)$$

The wind in the layer of air near the ocean surface can be expressed as a function of height, h, given the wind profile for the first few hundred meters. Given the friction velocity, (u^*), the divergence can be expressed as a function of height for neutral stability and integrated from the surface upward. This will be done after the fields for the wind stress and the curl of the wind stress are found.

The Monin-Obukhov theory and the concept of the drag coefficient given by equation (70) for a neutral atmosphere

$$C_{D10} = u_*^2/U_{10}^2 \tag{70}$$

where $$u_*^2 = \tau/\rho = - \langle u' w' \rangle \tag{71}$$

have been the methods used to try to understand the turbulent boundary layer over the ocean. Many different sets of measurements have been made in order to try to determine the relationship between wind stress and the wind at 10 meters.

It is not relevant to this particular investigation to review the great many papers that have been written that describe the results of these many investigations. Reviews or some of these studies are given by Phillips (1977) and Neumann and Pierson (1966).

More recent results using more modern and more carefully calibrated instrumentation that cover a large range of wind speeds are those of Davidson, et al. (1981), Dittmer (1977), Smith (1980) and Large and Pond (1981). Low winds are covered by Davidson, et al. (1981), low and moderate winds, by Dittmer (1977) and moderate and high winds, by Smith (1980) and Large and Pond (1981).

Smith and Large and Pond used methods that measured $\langle u' w' \rangle$ directly as well as the dissipation in the Kolmogorov range which was than correlated with $\langle u' w' \rangle$ and U_{10}. All of the data obtained to determine the relationship between wind stress and U_{10} scatter when plotted either as τ/ρ versus U_{10} or as C_{10} versus U_{10}.

To investigate the problem in still one more way, an analysis was made as a term paper*, by Vera, of the data provided by W. G. Large and extracted from the publications of Davidson, et al. and Dittmer. For neutral stability, the data were of the form n_i, $(\tau/\rho)_i$, U_{10i}, for a data set that ranged from light winds of 1 m/s to winds of 27 m/s. The higher winds have smaller values

---

*Vera, Emilio E., A Study of Curve Fitting Procedure for the Wind Versus Wind Stress Relationship. Term paper for an Oceanography Course, The City College of New York.

for n_i (where n_i represented the number of individual runs in a restricted range of wind speeds that were averaged to produce the u_*^2 and U_{10} values) and weight the fit less strongly than moderate and low winds.

The need is for the most accurate possible prediction of the wind stress given the wind at ten meters. Instead of first finding C_{10}, it seems that it would be more direct to minimize the error in predicting the wind stress from the wind speed from the available data as in equation (72).

$$Q = \sum_{1}^{N} (n_i (\tau/\rho)_i - A\, U_{10i} = B\, U_{10i}^2 - C\, U_{10i}^3)^2 \qquad (72)$$

This is accomplished by finding those values of A, B and C that minimize Q by requiring that $\partial Q/\partial A = 0$ $\partial Q/\partial B = 0$ and $\partial Q/\partial C = 0$ which yields equations (73).

$$\begin{vmatrix} \sum n_i U_{10i}^2 & \sum n_i U_{10i}^3 & \sum n_i U_{10i}^4 \\ \sum n_i U_{10i}^3 & \sum n_i U_{10i}^4 & \sum n_i U_{10i}^5 \\ \sum n_i U_{10i}^4 & \sum n_i U_{10i}^5 & \sum n_i U_{10i}^6 \end{vmatrix} \begin{vmatrix} A \\ B \\ C \end{vmatrix} = \begin{vmatrix} \sum n_i U_{10i} (\tau/\rho)_i \\ \sum n_i U_{10i}^2 (\tau/\rho)_i \\ \sum n_i U_{10i}^3 (\tau/\rho)_i \end{vmatrix} \qquad (73)$$

A good fit was found for the data that were used in terms of equation (74).

$$u_*^2 = \tau/\rho = 10^{-3} (2.717\, U_{10} + 0.142\, U_{10}^2 + 0.0761\, U_{10}^3) \qquad (74)$$

Graphs of τ/ρ versus U_{10} for the averaged data of Large and as extracted from the two other sources are plotted on linear scales in Figure 3 and on logarithmic scales in Figure 4. Figure 4 shows how the slope of the τ/ρ versus U_{10} relationship varies from one to almost three as the wind speed increases.

Vera also investigated the possibility that some power law as in equation (75) might fit the data better.

$$\tau/\rho = \alpha U^{\beta} \qquad (75)$$

It was found that no power law did as well as equation (74). As shown in

Figure 4 power laws can only be made to fit a portion of the data and fail outside of a restricted range. Equation (74) will consequently be used in this investigation subject to the comment made in the introduction. Given any equation that relates wind stress and the wind at ten meters, the analysis that follows can still be applied.

The SASS data are for winds at 19.5 meters. To calculate the stress it is necessary to know the wind at 10 meters. The wind at 10 meters is

$$U(10) = \frac{u_*(U_{10})}{\kappa} \ln (10/z_o) \tag{76}$$

,since $u_*(U_{10})$ is known as a function of U_{10}, which implies z_o, and at 19.5 meters it is

$$U(19.5) = \frac{u_*(U_{10})}{\kappa} \ln (19.5/z_o) \tag{77}$$

so that

$$U(19.5) = U(10) + \frac{u_*(U_{10})}{\kappa} \ln (19.5/10) \tag{78}$$

When U(10) is varied in convenient increments, a table of U(19.5) versus U(10) can be generated. Given a value of U(19.5), interpolation yields a value of U(10) to be in the calculation of τ/ρ and if ρ is known τ.

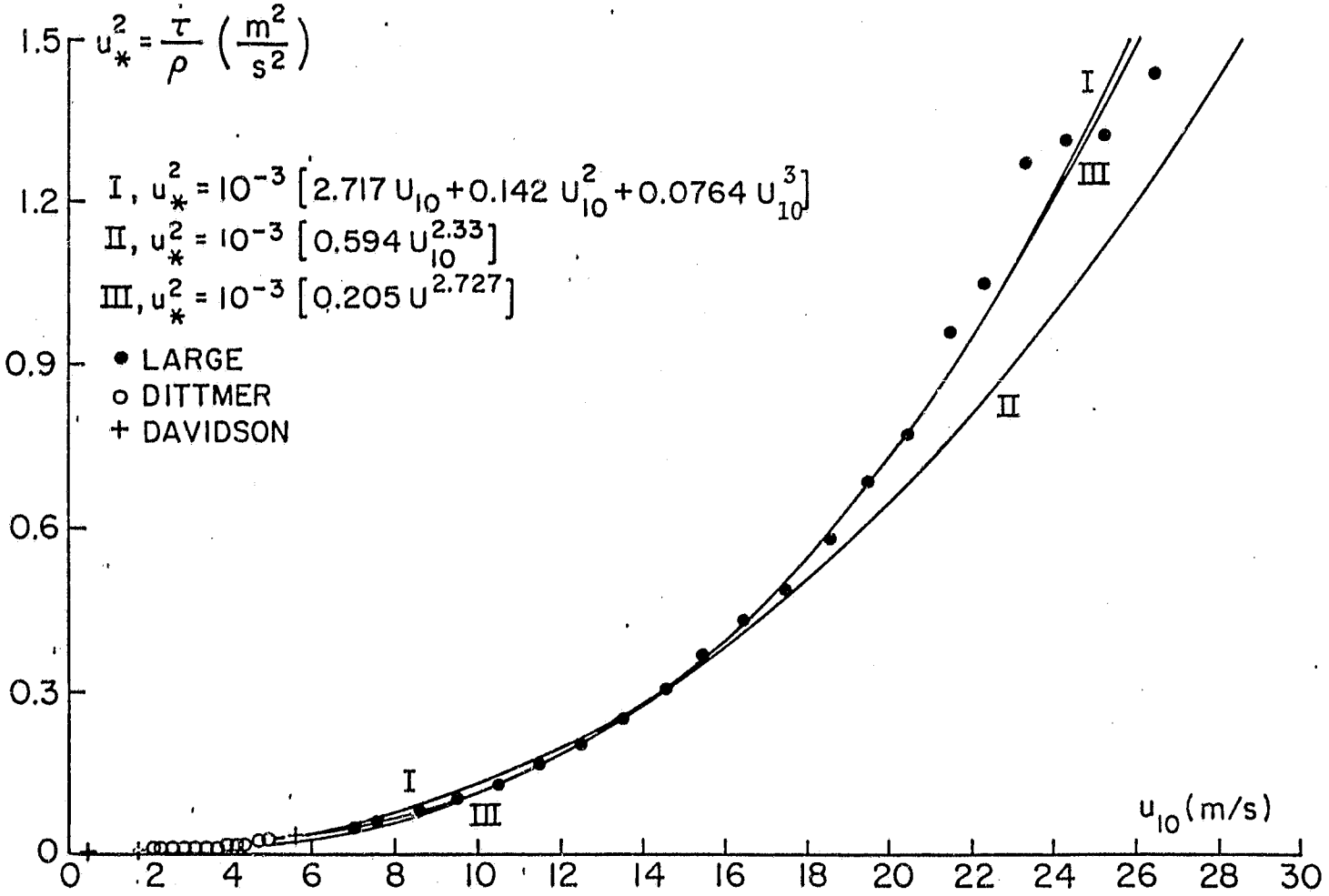

FIGURE 3 u_*^2 Versus U_{10} on Linear Scales

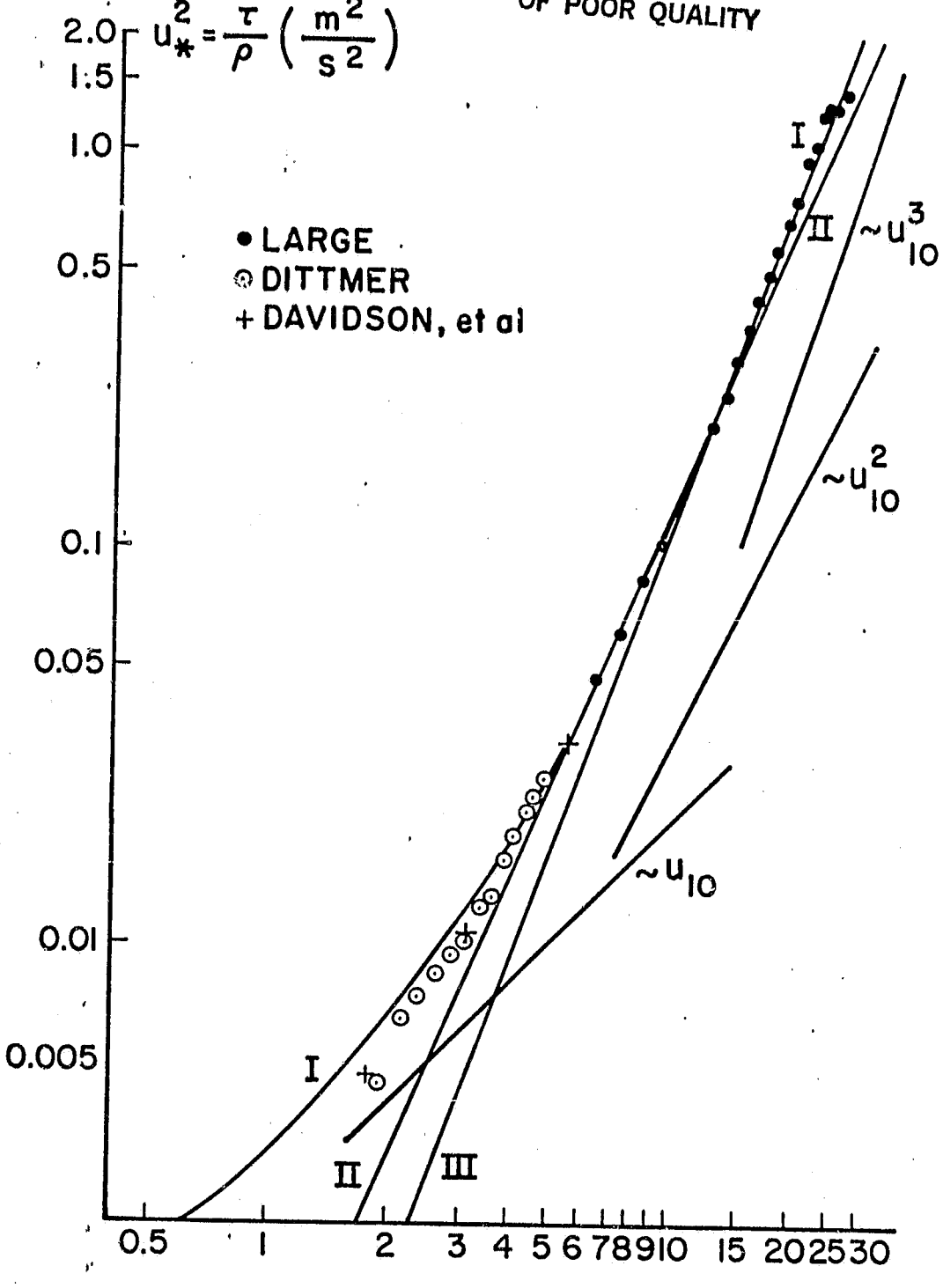

FIGURE 4 u_*^2 Versus U_{10} on logarithmic Scales.

THE CALCULATION OF THE STRESS

Given the individual SASS winds scattered over a SEASAT swath, one might consider taking the basic data, reducing the wind to 10 m., calculating the stress and deriving such quantities as the curl of the stress at whatever resolution is available. For many reasons, this line of analysis will lead to dubious results.

Aspects of the difficulty can be illustrated by calculating a super-observation wind stress two different ways: The first is by calculating the stress at each SASS point averaging the stresses, and analysing the statistics, and the second is by using the results of equations (5) to (10), reinterpreting them and calculating the stress and its statistics from the vector averaged winds.

A new coordinate system is needed as a first step. Let two great circles intersect at λ_o, θ_o with one in the direction $\bar{\chi}$ from (5) and the other at right angles to it, and let distance along the first be given by G_1 (degrees) and along the second by G_2 (degrees). A coordinate transformation would be possible as in the divergence analysis as a last step when needed.

The wind from the SASS at any point in the two degree by two degree square would then be represented by (79) and (80).

$$V_{Pi} = U_p(\lambda_i, \theta_i) + \Delta U_i \tag{79}$$

$$V_{Ni} = V_N(\lambda_i, \theta_i) + \Delta V_i \tag{80}$$

where in turn

$$\Delta U_i = \frac{\partial\, U(\lambda_o, \theta_o)}{\partial G_1} \Delta G_{1i} + \frac{\partial U\,(\lambda_o,\ \theta_o)}{\partial G_2} \Delta G_{2i}$$

$$+ t_{1i}\ \Delta U_m + t_{2i}\ \Delta U_c \tag{81}$$

and

$$\Delta V_i = \frac{\partial V(\lambda_o, \theta_o)}{\partial G_1}\ \Delta G_{1i} + \frac{\partial V(\lambda_o, \theta_o)}{\partial G_2}\ \Delta G_{2i}$$

$$+ t_{3i}\ \Delta V_m + t_{4i}\ \Delta V_3 \tag{82}$$

In (81) and (82), any residuals from the gradients of the wind from the average values of ΔG_{1i} and ΔG_{2i} can be removed for superobservations as shown by equation (44). The terms ΔU_m, ΔU_c, ΔV_m and ΔV_c have a new meaning and must be interpreted in terms of the analysis given by Pierson (1982). The terms, ΔU_m and ΔV_m, represent the contribution to a particular SASS wind of the mesoscale variability of the wind for each SASS cell. The terms, ΔU_c and ΔV_c, represent the communication noise error in the measurement made by SASS for each pair of cells. They are in the form of standard deviations to be multiplied by random numbers, t_{1i}, t_{2i}, t_{3i}, and t_{4i}, from zero mean unit variance probability density functions. This random error is a not too well known function of incidence angle, aspect angle, polarization and neutral stability wind speed. For winds near upwind, downwind and cross wind, the communication noise error can be substantial and the mesoscale contribution is a strong function of wind speed. If finite differences are used to calculate divergences over smaller distances with the original SASS winds, the last two terms in (81) and (82) dominate the calculation of the gradients to find differences as opposed to the analysis given previously for a superobservations. The SASS GOASEX data do not provide a way to separate these two effects. Even more discouraging results are obtained when these individual observations are used to obtain wind stress and wind stress curl.

From (79) and (80), the magnitude of the wind at $\lambda_i \theta_i$ is

$$|V_i| = ((U_p(\lambda_i,\theta_i) + \Delta U_i)^2 + (\Delta V_i)^2)^{\frac{1}{2}} \tag{83}$$

and so the magnitude of τ/ρ is

$$\tau/\rho\ (\lambda_i,\ \theta_i) = A|V_i| + B|V_i|^2 + C|V_i|^3 \tag{84}$$

When expanded to second order in ΔU_i and ΔV_i, this becomes (85)

$$\begin{aligned}\tau/\rho(\lambda_i,\theta_i) &= AU_p(\lambda_i,\theta_i) + B(U_p(\lambda_i,\theta_i))^2 + C(U_p(\lambda_i,\theta_i))^3 \\ &+ (A + 2BU_p(\lambda_i,\theta_i) + 3C(U_p(\lambda_i,\theta_i))^2)\ U_i \\ &+ (B + 3CU_p(\lambda_i,\theta_i))\ (\Delta U_i)^2 \\ &+ (B + \tfrac{3}{2} CU_p(\lambda_i,\theta_i))(\Delta V_i)^2 \end{aligned} \tag{85}$$

The squares of ΔU_i and ΔV_i involve terms of the form,

$$t_{1i}^2 (\Delta U_m)^2 + t_{2i}^2 (\Delta U_c)^2$$

that do not fluctuate about zero and that do not average to zero. Moreover they are amplified at high winds by the wind speed. Individual values of the wind stress calculated from the SASS data thus appear to be somewhat untrustworthy.

If the N winds used to generate the superobservation wind are each used separately, N values of τ/ρ can be obtained and these N magnitudes of τ/ρ can be averaged. The expected value of this average is given by (86) where $U = U(\lambda_o, \theta_o)$.

$$\begin{aligned}
\mathcal{E}\ (\tau/\rho(\lambda_i,\theta_i)) &= A\bar{U}_p + B\bar{U}_p^2 + C\bar{U}_p^3 \\
&+ (A + 2B\bar{U}_p + 3C\bar{U}_p^2)\left(\frac{\partial \bar{U}_p}{\partial G_1}\overline{\Delta G}_1 + \frac{\partial \bar{U}_p}{\partial G_2}\overline{\Delta G}_2\right) \\
&+ (B+3C\bar{U}_p)^2 \left(\left(\frac{\partial \bar{U}_p}{\partial G_1}\right)^2 \mathrm{VAR}\,\Delta G_1 + \left(\frac{\partial \bar{U}_p}{\partial G_2}\right)^2 \mathrm{VAR}\Delta G_2 + 2\frac{\partial \bar{U}_p}{\partial G_1}\frac{\partial \bar{U}_p}{\partial G_2}\,\mathrm{COV}\,\Delta G_1\,\Delta G_2\right) \\
&+ (B+\tfrac{3}{2}C\bar{U}_p)^2 \left(\left(\frac{\partial \bar{V}_p}{\partial G_1}\right)^2 \mathrm{VAR}\,\Delta G_1 + \left(\frac{\partial \bar{V}_p}{\partial G_2}\right)^2 \mathrm{VAR}\Delta G_2 + 2\frac{\partial \bar{V}_p}{\partial G_1}\frac{\partial \bar{V}_p}{\partial G_2}\,\mathrm{COV}\,\Delta G_1\,\Delta G_2\right) \\
&+ (B+3C\bar{U}_p)(B+\tfrac{3}{2}C\bar{U}_p)\left(\frac{\partial \bar{U}_p}{\partial G_1}\frac{\partial \bar{V}_p}{\partial G_2}\mathrm{VAR}\Delta G_1 + \frac{\partial \bar{U}_p}{\partial G_2}\frac{\partial \bar{V}_p}{\partial G_2}\mathrm{VAR}\,\Delta G_2 + \frac{\partial \bar{U}_p}{\partial G_1}\frac{\partial \bar{V}_p}{\partial G_2}\right. \\
&\left. + \frac{\partial \bar{U}_p}{\partial G_2}\frac{\partial \bar{V}_p}{\partial G_1}\right)\,\mathrm{COV}\,\Delta G_1\,\Delta G_2 \\
&+ (\Delta U_m)^2 + (\Delta U_c)^2 + (\Delta V_m)^2 + (\Delta V_c)^2 \qquad (86)
\end{aligned}$$

Although the average can in theory be corrected by various estimates of the numerous terms that produce a bias, the errors of various kinds in the original SASS data are quite large. Additional terms to third order would introduce even larger effects since the cube of the wind speed is involved. Variability in direction produces even more intricate results.

The variance of the data would be found from $\mathcal{E}\ (\tau/\rho\ (\lambda_i,\theta_i) - \tau/\rho\ (\lambda_i,\theta_i))^2$ and yields terms involving the squares of ΔU_m, ΔU_c, ΔV_m and ΔV_c multiplied

functions of U, A, B and C. This variance would be reduced by N^{-1} when used in calculations involving the wind stress field but proceeding in this way leads to intricate correction procedures and the need to correct for large effects.

In contrast consider the average wind for the N values around λ_o, θ_o as given by (29) and (30) which could be corrected for the effects of a gradient by finding (45) and its counterpart for $\bar{V}(\lambda_o, \theta_o)$. The standard deviations caused only by the combined effects of mesoscale effects and communication noise could be found from (54) through (57) and returning to vectors parallel and normal to the direction $\bar{\chi}$.

The result would be four numbers at λ_o, θ_o, namely $\bar{\chi}$, and

$$\bar{V}_P = \bar{U}_p(\lambda_o, \theta_o) + t_5 N^{-\frac{1}{2}} \nabla U_{mc} \tag{87}$$

$$\bar{V}_N = t_6 N^{-\frac{1}{2}} \Delta V_{mc} \tag{88}$$

where the combined residual effects of mesoscale variability and communication noise have been reduced by $N^{-\frac{1}{2}}$ to describe the sampling variability of the mean. Failure to correct for the contribution from the synoptic scale gradients and using the values found at $\lambda_o + \overline{\Delta\lambda}$, $\theta_o + \overline{\Delta\lambda}$ with standard deviations reduced by $N^{-\frac{1}{2}}$ would also give much more stable results.

For a superobservation, substitute (87) and (88) into (85) and the result is ´89).

$$\begin{aligned} \tau/\rho(\lambda_o, \theta_o)_s = {} & A\bar{U}_p + B\bar{U}_p^2 + C\bar{U}_p^3 \\ & + (A + 2B\bar{U}_p + 3C\bar{U}_p^2)\, t_5 N^{-\frac{1}{2}} \Delta U_{mc} \\ & + (B + 3C\bar{U}_p)\, t_5^2 N^{-1} (\Delta U_{mc})^2 \\ & + (B + \tfrac{3}{2} C\bar{U}_p)\, t_6^2 N^{-1} (\Delta V_{mc})^2 \end{aligned} \tag{89}$$

Over a one degree field the uncertainty in the value of $\tau/\rho(\lambda_o, \theta_o)$ is greatly reduced by the factor $N^{-\frac{1}{2}}$ and the bias is even more strongly reduced by N^{-1}. Similar effects occur for direction.

It appears to suffice to process the data in an even simpler way for the center of the swath. The superobservation wind data can be reduced to 10 meters instead of the individual winds. The value of $U_*^2 = \tau/\rho(\lambda_o, \theta_o)$ can be found from

$$\bar{\tau}/\rho\ (\lambda_o,\ \theta_o;\ \bar{U}_p) = A\ \bar{U}_p + B\ \bar{U}_p^2 + C\ \bar{U}_p^3 \tag{90}$$

The variability of the stress in the direction $\bar{\chi}$ can be found from (27), (31) and (30) after correction by (54) to (57) and after correction to 10 meters,

$$\Delta_p(\tau/\rho) = \tau/\rho\ (\bar{U}_p + N^{-\frac{1}{2}}\ \Delta U_{mc}) - \tau/\rho\ (\bar{U}_p) \tag{91}$$

The variability normal to $\bar{\chi}$ that would give a vector stress with the same direction as the vector sum of (87) and (88) with $t_5 = 0$ and $t_6 = 1$ is given by (92)

$$\Delta_N(\tau/\rho) = \tau/\rho(\bar{U}_p)\ \left(\frac{N^{-\frac{1}{2}}\ \Delta V_{mc}}{\bar{U}_p}\right) \tag{92}$$

The stress is represented by

$$\tau/\rho_1(\lambda_o,\theta_o)_{Ps} = \tau/\rho(\bar{U}_p) + t_7\ \Delta_p(\tau/\rho) \tag{93}$$

$$\tau/\rho(\lambda_o,\theta_o)_{Ns} = t_8\ \Delta_N(\tau/\rho) \tag{94}$$

with orthogonal components in the direction, $\bar{\chi}$ and normal to $\bar{\chi}$. These in turn can be resolved into east-west and north-south components and processed in the same way as the winds.

The curl of the horizontal vector wind stress is found by first multiplying equations (93) and (94) by $\rho(\lambda_o,\theta_o)$ which can be found from the air temperature and the atmospheric pressure at the sea surface and then computing the north-south and east-west components of the stress plus the appropriate $\Delta\tau$'s. Values of $\rho(\lambda_o,\theta_o)$ vary about 1.25 kg/m^2. In spherical coordinates,

$$\text{CURL}(\vec{\tau}_h) = \frac{1 \cos\theta}{R}\left(\frac{\partial \tau_{(\theta)s}}{\partial \lambda} - \frac{\partial(\cos\theta\, \tau_{(\lambda)s})}{\partial \theta}\right)$$

$$= \frac{1 \cos\theta}{R}\left(\frac{\partial \tau_{(\theta)s}}{\partial \lambda} - \cos\theta \frac{\partial \tau_{(\lambda)s}}{\partial \theta} + \sin\theta\, \tau_{(\lambda)s}\right) \qquad (95)$$

where $\tau_{(\theta)s}$ and $\tau_{(\lambda)s}$ are the north-south and east-west vector components of $\vec{\tau}_s$. If for example

$$\tau_{(\theta)s}(\lambda_o,\theta_o) = \bar{\tau}_{(\theta)}(\lambda_o,\theta_o) + t_9\,\Delta\tau_1 + t_{10}\,\Delta\tau_2 \qquad (96)$$

$$\tau_{(\lambda)s}(\lambda_o,\theta_o) = \bar{\tau}_{(\lambda)}(\lambda_o,\theta_o) + t_{11}\,\Delta\tau_3 + t_{12}\,\Delta\tau_4 \qquad (97)$$

and so on, the finite difference value of (95) is

$$\text{CURL}(\vec{\tau}_h)_s = \frac{4.5\cdot 10^{-6}}{(\cos\theta_o)}\Big\{\tau_{(\theta)s}(\lambda_o, +1, \theta_o) - \tau_{(\theta)s}(\lambda_o - 1, \theta_o)$$

$$- \cos\theta_o\,(\tau_{(\lambda)s}(\lambda_o, \theta_o + 1) - \tau_{(\lambda)s}(\lambda_o, \theta_o - 1)$$

$$+ 0.0349065 \sin\theta_o\, \tau_{(\lambda)s}(\lambda_o,\theta_o))\Big\} \qquad (98)$$

with dimensions of (newtons m^{-2}) m^{-1}.

Ten different random effects are found in the calculation. The expected value of the curl and the expected value of the variance of the curl are given by (99) and (100) where ten different $\Delta\tau$'s from the five different stresses that are used are needed for (100).

$$e\,(\text{CURL}\,(\vec{\tau}_h))_s = \frac{4.5\cdot10^{-6}}{(\cos\theta_o)}\Big[\bar{\tau}_{(\theta)}(\lambda_o + 1,\ \theta_o) - \tau_{(\theta)}(\lambda_o - 1,\ \theta_o)$$

$$- \cos\theta_o\,(\tau_{(\lambda)}(\lambda_o,\theta_o + 1) - \tau_{(\lambda)}(\lambda_o,\theta_o - 1))$$

$$+ 0.0349065\,\sin\theta_o\ \tau_{(\lambda)}(\lambda_o,\theta_o)\Big]$$

$$= \overline{\text{CURL}\,(\vec{\tau}_h)} \qquad (99)$$

$$\text{VAR}\,(\overline{\text{CURL}(\vec{\tau}_h)}) = \frac{2.025\cdot10^{-11}}{(\cos\theta_o)^2}\Big[(\Delta\tau(\lambda_o + 1,\ \theta_o)_2)^2$$

$$+ (\Delta\tau(\lambda_o - 1,\ \theta_o)_1^2 + (\Delta\tau(\lambda_o - 1,\ \theta_o)_2^2$$

$$+ (\cos\theta)^2\,((\Delta\tau(\lambda_o,\theta_o + 1)_3)^2 + \cdots\cdot)$$

$$+ 1.2184\cdot10^{-3}\,(\sin\theta_o)^2\,((\Delta\tau(\lambda_o,\theta_o)_1)^2 + \cdots)\Big] \qquad (100)$$

,where $\cdots\cdot$ the represents the additional terms needed to complete the full equation,

so that

$$(\text{CURL}\,\vec{\tau}_h)_s = \overline{\text{CURL}(\vec{\tau}_h)} + t(\text{VAR}(\text{CURL}(\vec{\tau}_h)))^{\frac{1}{2}} \qquad (101)$$

If the neutral wind profile is assumed to extend to the height, h_2, equation (65) can be rewritten and the result integrated from h_1, very near the sea surface where $W(R_o + h_1)$ is nearly zero at the synoptic scale, to h_2. In the limit, h_1 can be set to zero and the subcript, 2, can be omitted.

$$\int_{R_o + h_1}^{R_o + h_2} \frac{\partial}{\partial R}(R^2 W(R))\,dR = -\int_{R_o + h_1}^{R_o + h_2} R \,\mathrm{div}_2\, W_h \, dR \tag{102}$$

Many of the terms that arise and that enter into the finite difference calculation are negligable. Two turn out to be important and are effectively multiplied by terms that are constants as far as the integration is concerned. One is of the form given by equation (103).

$$\int_{h_1}^{h_2} (\mathrm{const}_1)\, dz = \mathrm{const}_1\, (h_2 - h_1) \tag{103}$$

and the other is (104)

$$\int_{h_1}^{h_2} \mathrm{const}_2\, \ell n(z/10)\, dz = \mathrm{const}_2 (h_2\, \ell n\, \frac{h_2}{10} - h_2 - h_1\, \ell n\, \frac{h_1}{10} + h_1) \tag{104}$$

By means of equations similar to (27), and following, with the wind reduced to 10 meters and with the standard deviations of the means, values for $\bar{V}_p$, ΔU and ΔV can be found at λ_o, θ_o.

Define

$$u_* = (A\bar{V}_p + B\bar{V}_p^2 + C\bar{V}_p^3)^{1/2} \tag{105}$$

$$\Delta u_{*p} = u_*(\bar{V}_p + \Delta U) = u_*(\bar{V}_p) \tag{106}$$

and $$\Delta u_{*N} = u_*(\bar{V}_p) \cdot (\Delta V / V_p) \tag{107}$$

Then $$V_p(z)_s = \bar{V}_p + \frac{u_*\, \ell n\, z/10}{\kappa} + t_1 \left(\Delta U + \frac{\Delta U_*\, \ell n\, z/10}{\kappa}\right) \tag{108}$$

$$V_N(z)_s = t_2 \left(\Delta V + \frac{\Delta U_{*N}\, \ell n\, z/10}{\kappa}\right) \tag{109}$$

The terms analogous to (33) to (40) are

$$U(z) = -(\bar{V}_p + \frac{u_* \ell n\ (z/10)}{\kappa})\ \sin \bar{\chi}$$

$$= \bar{U}(10) + \delta_1 U)\ \ell n\ z/10 \tag{110}$$

$$\bar{V}_z = -(\bar{V}_p + \frac{u_* \ell n\ (z/10)}{\kappa})\ \cos \bar{\chi}$$

$$= \bar{V}(10) + (\delta_1 V) \ell n\ (z/10) \tag{111}$$

$$\Delta U_1(z) = \Delta U_1 - \frac{\sin \bar{\chi}\ \Delta u_{*p}\ \ell n\ (z/10)}{\kappa}$$

$$= \Delta U_1 + (\delta_2 U_1)\ \ell n\ (z/10) \tag{112}$$

$$\Delta U_2(z) = \Delta U_2 - \frac{\cos \bar{\chi}\ \Delta u_{*N} \ell n\ (z/10)}{\kappa}$$

$$= \Delta U_2 + (\delta_2\ U_2) \ell n\ (z/10) \tag{113}$$

$$\Delta V_1(z) = \Delta V_1 - \frac{\cos \bar{\chi}\ \Delta u_{*p}\ \ell n\ (z/10)}{\kappa}$$

$$= \Delta V_1 + (\delta_2 V_1)\ \ell n\ (z/10) \tag{114}$$

$$\Delta V_2(z) = \Delta V_2 + \frac{\sin \bar{\chi}\ \Delta u_{*N}\ \ell n\ (z/10)}{\kappa}$$

$$\Delta V_2 + (\delta_2 V_2)\ \ell n\ (z/10) \tag{115}$$

The appropriate terms, all of which can be found for each grid point in the field, can be substituted into (71). After integration of (102) and simplification by the results implied by (103) and (104), the final result is equation (116), where the subscript on h_2 has been dropped. The ΔU's and so on, need to be found at the correct latitudes and longitudes.

$$\bar{w}\ (h)_s = \frac{4.5 \cdot 10^{-6} h}{\cos \theta_o} \Big[\bar{U}_{10}(\lambda_o + 1,\ \theta_o) + \delta_1 U(\lambda_o + 1, \theta_o) \cdot (\ell n \frac{h}{10} - 1)$$

$$- \bar{U}_{10}(\lambda_o - 1, \theta_o) - \delta_1 U(\lambda_o - 1, \theta_o) \cdot (\ell n \frac{h}{10} - 1) + t_1 (\Delta U_1 + \delta_2 u_* (\ell n \frac{h}{10} - 1))$$

$$+ t_2(\Delta U_2 + \delta_2 U_2(\ell n \frac{h}{10} - 1)) - t_3(\Delta U_1 + \delta_2 U_1(\ell n \frac{h}{10} - 1))$$

$$- t_4(\Delta U_2 + \delta_2 U_2(\ell n \frac{h}{10} - 1))$$

$$+ \cos\theta_o(\bar{V}_{10}(\lambda_o, \theta_o + 1) + \delta_1 V(\lambda_o, \theta_o + 1)(\ell n \frac{h}{10} - 1)$$

$$- \bar{V}_{10}(\lambda_o, \theta_o - 1) - \delta_1 \bar{V}(\lambda_o, \theta_o - 1)(\ell n \frac{h}{10} - 1) + \cdots\cdots)$$

$$+ 0.0349065 \sin\theta_o(\bar{V}_{10}(\lambda_o, \theta_o) + \cdots\cdots) \Big] \qquad (116)$$

At h = 200 meters, $\ell n \frac{h}{10} - 1$ is 2.0 and (117) becomes (118) in ms^{-1}.

$$\mathbb{w}(200)_s = \frac{9.10^{-4}}{\cos\theta_o} \Big[\bar{U}_{10}(\lambda_o + 1, \theta_o) + 2(\delta_1 U(\lambda_o + 1, \theta_o)) + \cdots$$

$$+ \cos\theta_o (\bar{V}_{10}(\lambda_o, \theta_o + 1) + 2(\delta_1 V(\lambda_o, \theta_o + 1) + \cdots$$

$$+ 0.0349065 \sin\theta_o (\bar{V}_{10}(\lambda_o, \theta_o) + 2\delta_1 V(\lambda_o, \theta_o))$$

$$+ \cdots\cdot) \Big] \qquad (117)$$

As in preceding analyses,

$$\mathbb{w}(200)_s = \bar{\mathbb{w}}(200) + t\,\Delta\bar{\mathbb{w}}(200) \qquad (118)$$

which can be evaluated in a way exactly similar to previous results.

As a note in passing, there is not much difference between (105), (106) and (107) and (90), (91) and (92). The computation of errors for the specific application is made simpler by the choice that was made. From

$$u_* + \Delta u_* = (u_*^2 + (\Delta u_*^2))^{\frac{1}{2}} = u_*(1 + (\Delta u_*^2)/u_*^2)^{\frac{1}{2}}$$

$$= u_*(1 + (\Delta u_*^2)/2u_*^2) = u_* + (\Delta u_*^2)/2u_* \qquad (119)$$

it can be seen that two different ways to find Δu_* yield nearly the same quantity.

INDEPENDENCE AND COVARIANCES

The reasons for the variability of one SASS pair of backscatter values compared to another pair are basically uncorrelated and random. The mean wind speed and the mean direction for a superobservation are perturbed by two independent and uncorrelated random effects, one parallel to the wind and one normal to it. A correlation becomes evident when resolving the superobservation into east-west and north-south components. A superobservation has been based on data from a 2^{o} by 2^{o} square, and once the effect of synoptic scale gradients are removed (which involves SASS values scattered randomly over the square from as far away as $\lambda_o \pm 2$ and $\theta_o \pm 2$), the estimate of the standard deviation of the mean is based on a sample of independent random variables. The choice of grid point spacing for superobservations for future systems remain a matter to be investigated and is a function of the model to be used and of the scatterometer that obtained the data. A very coarse resolution model in the horizontal would require a more careful treatment of gradients.

The use of overlapping squares at a one degree resolution introduces correlations between the estimates of the winds and the standard deviation of the variability simply because the same values are used in different estimates. Every other grid point in the east-west or north-south direction is independent and those located diagonally (for example, λ_o, θ_o to λ_o+1, θ_o+1) are weakly correlated. Smoothness in the wind field can be judged by inspecting every other point in the grid.

For the calculation of the divergence, the vertical velocity at h and the curl of the wind stress, the analysis becomes more complex. Some particular SASS speeds and directions can make contributions to the means plus standard deviations of three of the five terms that enter into the calculation. (The additional complexity introduced by (45) is not considered).

Equations (69) and (118) are essentially statistics formed from a linear weighted combination of the original data. Equation (100) is a pseudo-linearized plus non linear weighted combination of the original data.

Correlations do not do much damage in the estimation of means, but they can affect estimates of variances and standard deviations. The contribution of a particular SASS value to the final estimate of the divergence can be traced through the entire analysis. The value for the difference between two estimates of the east-west component so as to find $\partial U/\partial\lambda$ is calculated from completely different east-west components of the SASS values and thus the numbers on which the estimate is based are independent. The north-south difference so as to find $\partial V/\partial\theta$ is based on completely different north-south components of the SASS values weighed by a cosine and are also found from completely different values and thus the estimate is based on independent data.

For the calculation of the divergence as in (69) and quantities such as (101) and (119), the full expression is, however, somewhat more complicated and merits a more complete analysis. In Figure 1, the one degree squares that contain SASS values that enter into the evaluation of (74) are numbered from one to twelve. The values of $\bar{U}\ (\lambda_o,\theta_o)$ and $\bar{V}\ (\lambda_o,\theta_o)$ (and so on) are partially obtained from SASS values in squares 4, 5, 8, and 9. The wind for the point, λ_o, θ_o, was represented by equations (60) and (61). Let N equal $N = N_4 + N_5 + N_8 + N_9$, and then the term $\sum_1^N t_i\ \Delta U_i'$ can be represented by (120).

$$\sum_1^N t_i\ \Delta U_1 \tilde{=} \sum_1^{N_4} t_{i,4}\ \Delta U_{1,4} + \sum_1^{N_5} t_{i,5}\ \Delta U_{1,5} + \sum_1^{N_8} t_{i,8}\ \Delta U_{1,8} + \sum_1^{N_9} t_{i,9}\Delta U_{1,9} \qquad (120)$$

where the t's on the RHS are independent and the second subscript represents the one degree square containing the SASS value. The expected value of each side is zero and the expected value of the square of each side is

$$\mathcal{E}\left(\sum_1^{N_4} t_{1,4}\ \Delta U_{1,4} + \sum_1^{N_5} t_{1,5}\ \Delta U_{1,5} + \sum_1^{N_8} t_{1,8}\ \Delta U_{1,8} + \sum_1^{N_9} t_{1,9}\ \Delta U_{1,9}\right)^2$$

$$\tilde{=} 4\ \left(\frac{N}{4}\ (\Delta U_1')\right)^2 \qquad (121)$$

where the assumption that the error properties are the same in all four squares is made.

All of the contributions from each of the squares numbered in Figure 1 can be identified by a double subscript notation as above. The analysis can

be carried through keeping track of the dependence of $\Delta U_1'$ and $\Delta V_1'$ and of $\Delta U_2'$ and $\Delta V_2'$ throughout the finite difference calculation.

The contribution to the divergence from squares, 4, 5, 8 and 9 come from terms involving the gradients of U_s and V_s and value of V_s at λ_o, θ_o. For the $\Delta U_1'$ and $\Delta V_1'$ terms in (60) and (61) a part of their contribution can be represented by (122) where α' is the coefficient of the sine term in (67).

$$\begin{aligned}\text{Contribution} = {} & t_{1,5}\, N_5^{-\frac{1}{2}} (\Delta U'_{1,5} + \cos\theta_o\, \Delta V'_{1,5} + \alpha' \sin\theta_o\, \Delta V'_{1,5}) \\ & + t_{1,4}\, N_9^{-\frac{1}{2}} (\Delta U'_{1,9} - \cos\theta_o\, \Delta V'_{1,9} + \alpha' \sin\theta_o\, \Delta V'_{1,9}) \\ & + t_{1,4}\, N_4^{-\frac{1}{2}} (-\Delta U'_{1,4} + \cos\theta_o\, \Delta V'_{1,4} + \alpha' \sin\theta_o\, \Delta V'_{1,4}) \\ & + t_{1,8}\, N_8^{-\frac{1}{2}} (-\Delta U'_{1,8} - \cos\theta_o\, \Delta V'_{1,8} + \alpha' \sin\theta_o\, \Delta V'_{1,8}) \qquad (122)\end{aligned}$$

The expected value of this contribution to the divergence is zero. The expected value of $t_{1,5}^2$, $t_{1,9}^2$, $t_{1,4}^2$ and $t_{1,8}^2$ are one. The squares of the terms in parentheses give the terms found in (73) subject to the reasonable assumption of (121) and what it implies plus twelve cross product terms. The signs of the cross products terms are such that two of four similar terms have positive signs and two have negative signs. The cross correlation between $\bar{U}$ and $\bar{V}$ when estiamted from scattered SASS values will consequently cancel out and be close to zero in the estimate of the variability of the divergences as in (73). Although the terms in (71) as identified by t_1 to t_{10} are not strictly independent, this analysis shows that (68) and consequently (69), is essentially correct. The same conclusions are also valid for (99), (100), (101), (116), (117) and (118).

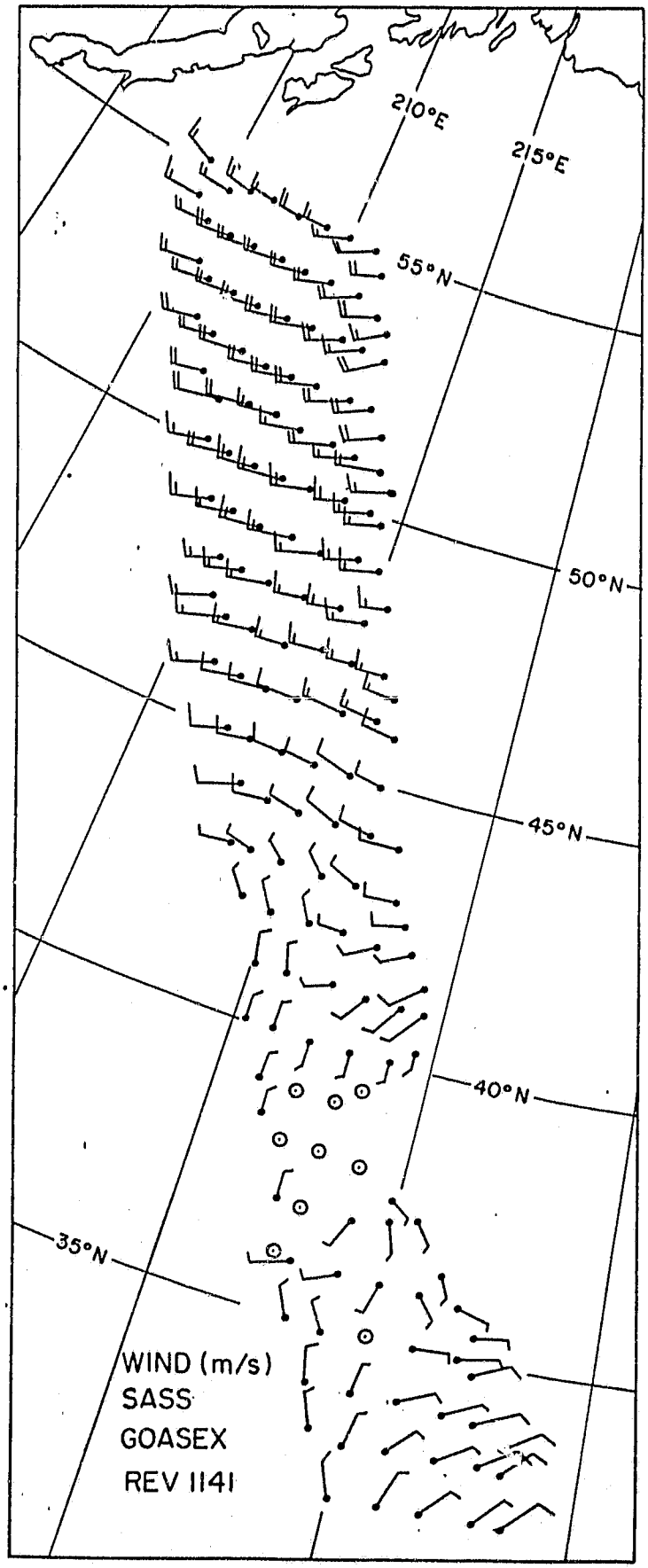

Arrows Fly with the Wind.
Barbs Proportional to Wind Speed.
Full Barb Equals 10 m/s.

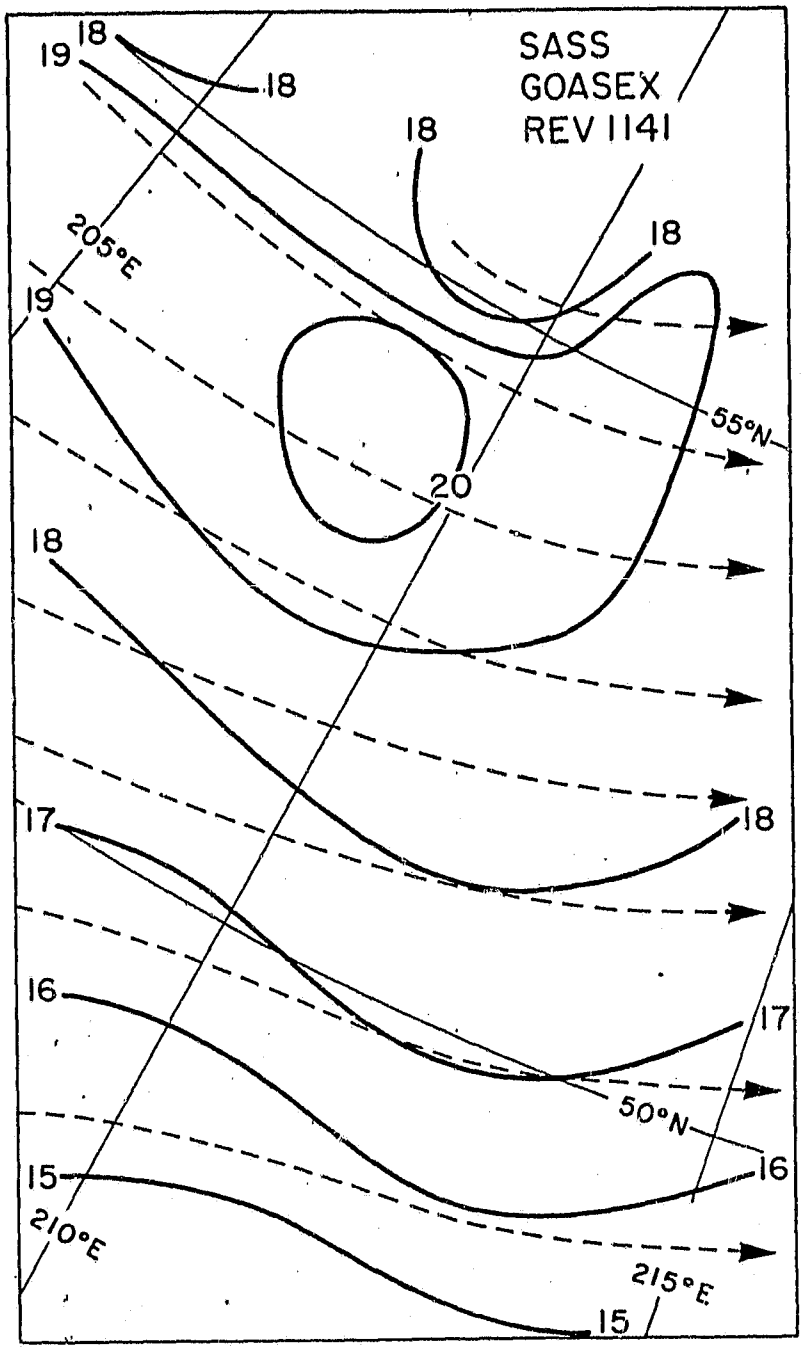

Solid Lines Isotachs
Dashed Lines Streamlines

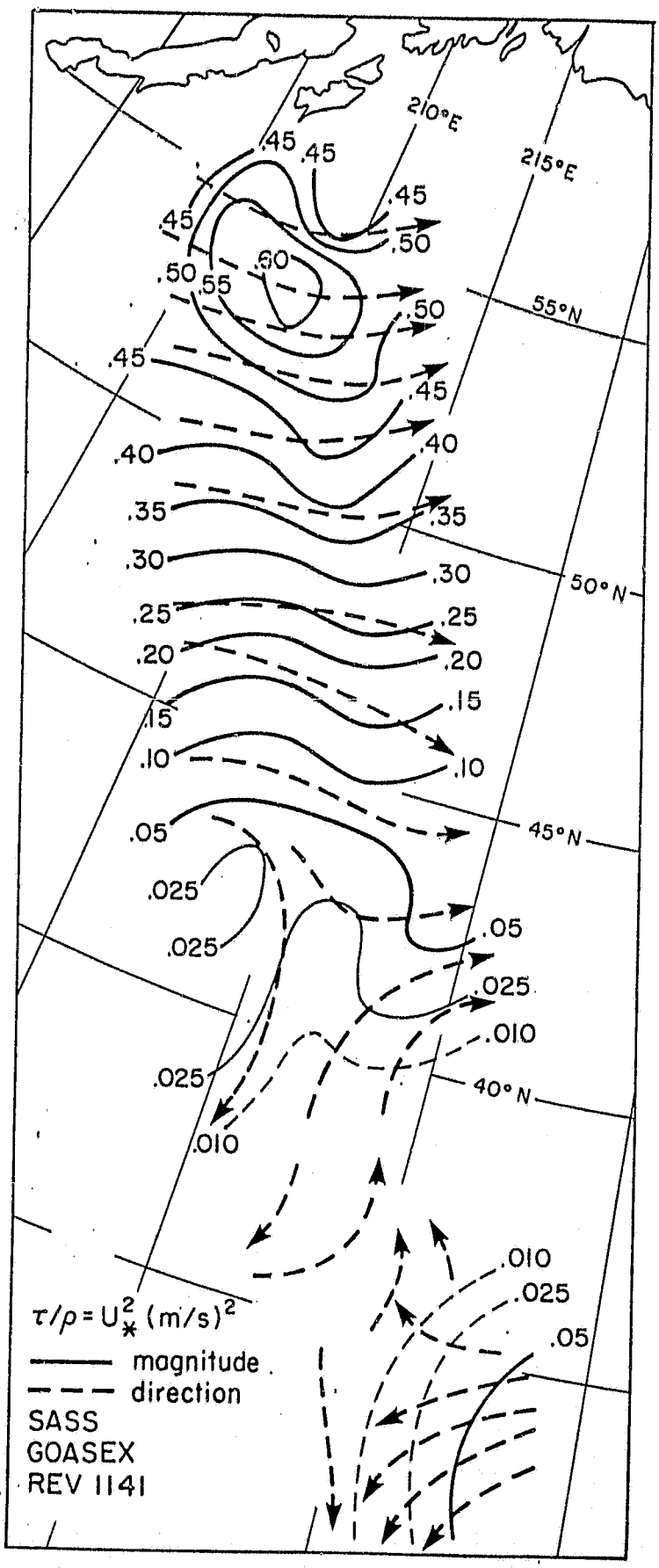

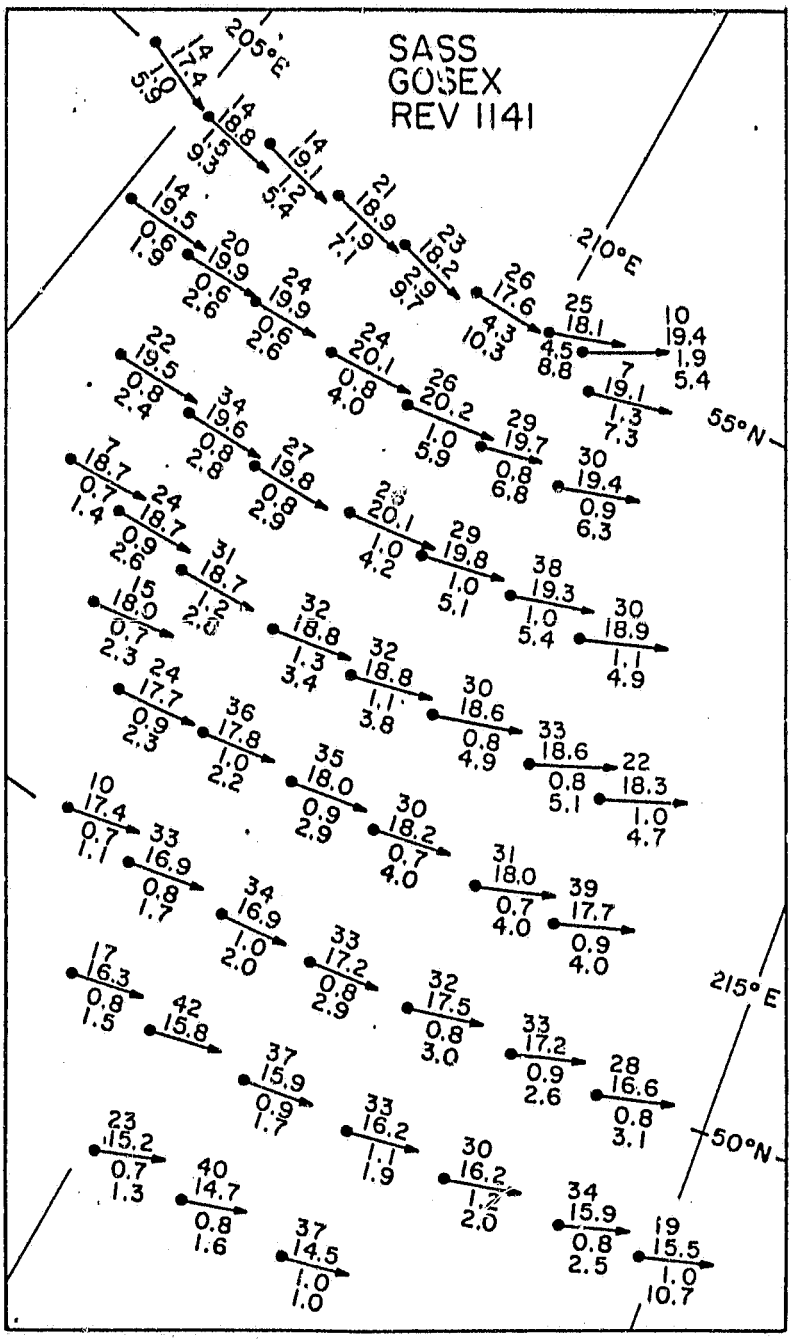

Top Left: SAMPLE SIZE
Top Right: $\overline{V}_P$
Bottom Left: ΔV_P
Bottom Right: ΔV_N
Multiply ΔV_P and ΔV_N by $N^{-\frac{1}{2}}$ to get Standard Deviations of the Mean.

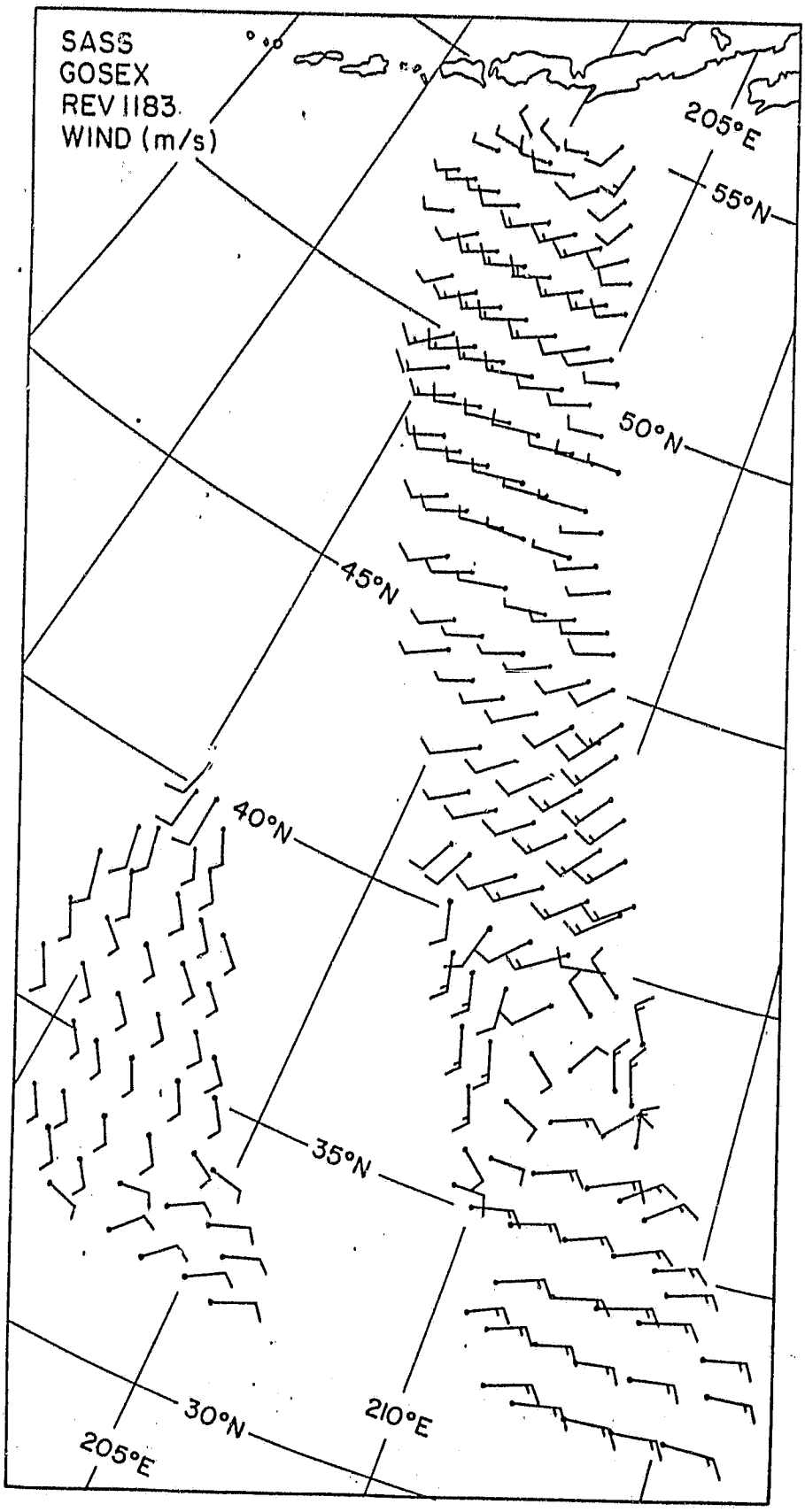

Arrows fly with the Wind, Barbs proportional to Wind Speed. Full Barb Equals 10 m/s.

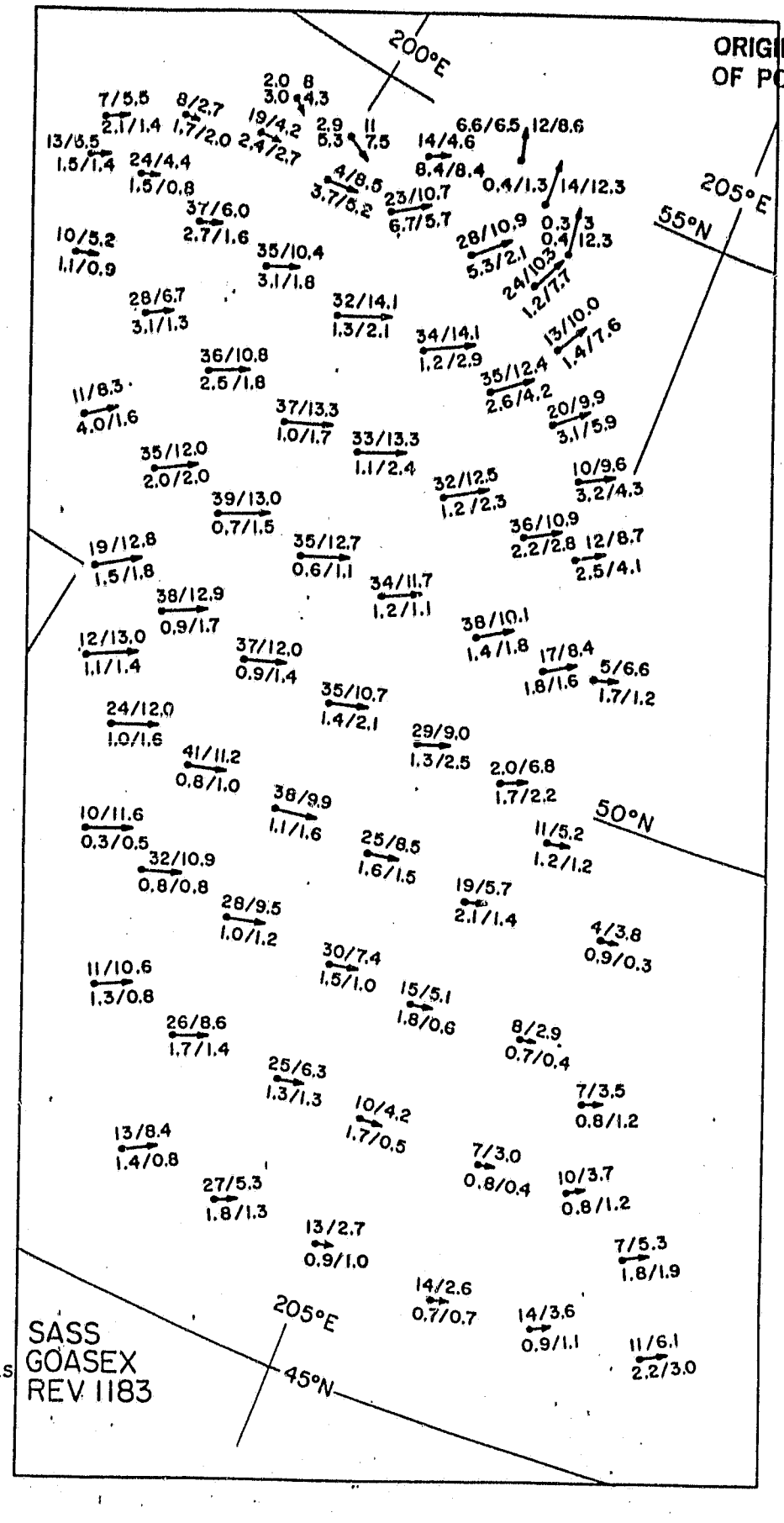

Top Left: SAMPLE SIZE.

TOP Right: $\overline{V}_p$

Bottom Left: ΔV_p

Bottom Right: ΔV_N

Multiply ΔV_p and ΔV_N by $N^{-\frac{1}{2}}$ to get Standard Deviations of the Mean.

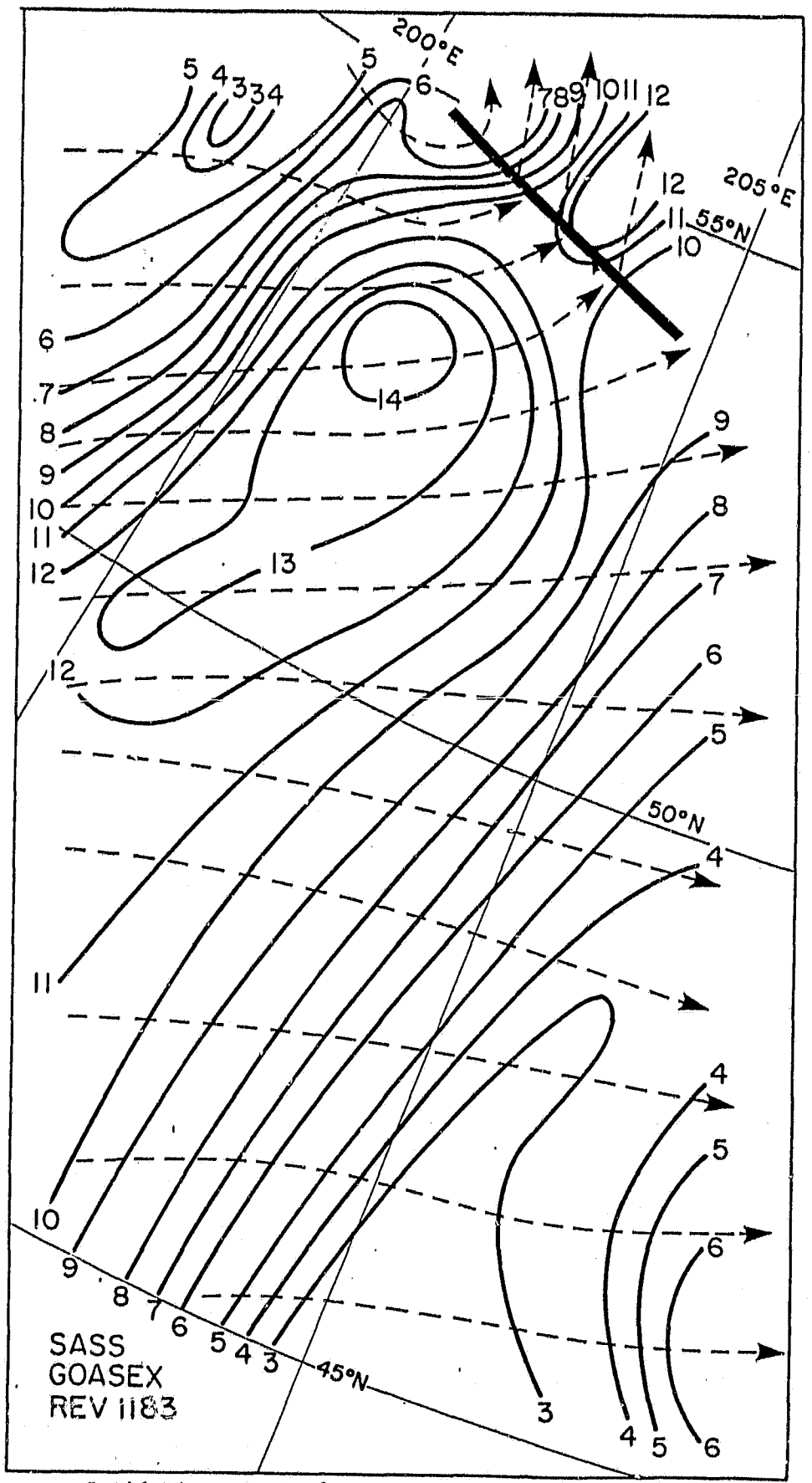

——— Solid Lines Isotachs
------- Dashed Lines Streamlines

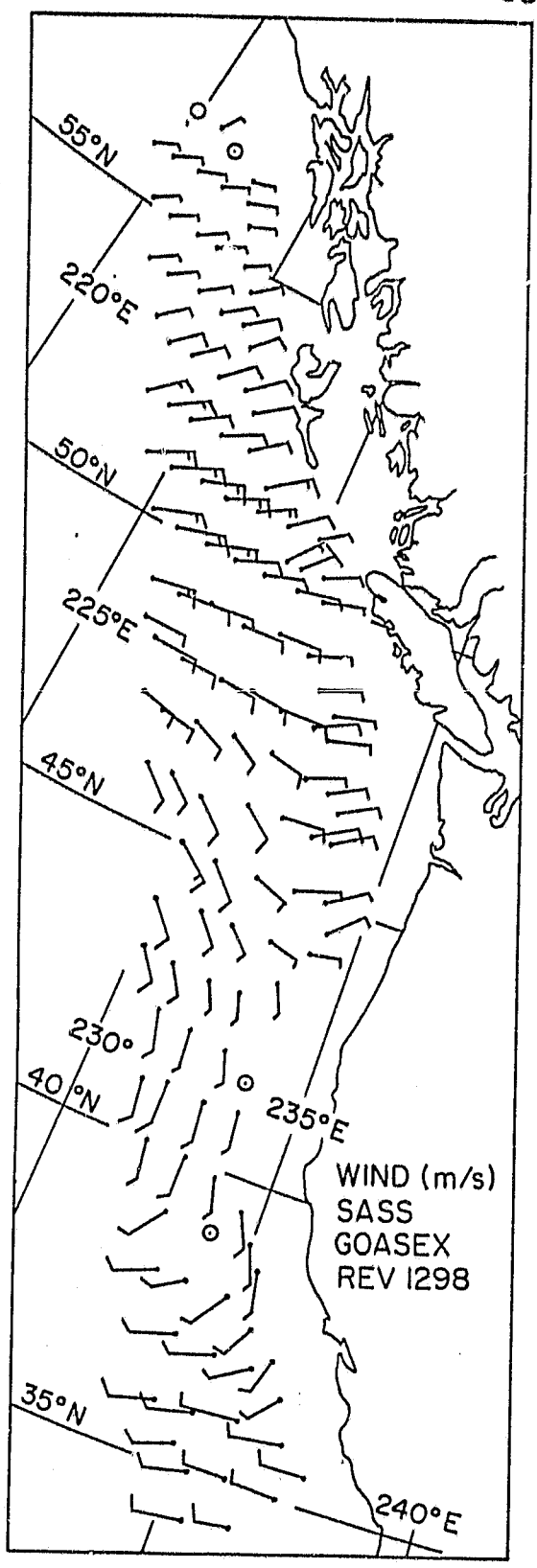

Arrows Fly with the Wind.
Barbs Proportional to Wind Speed.
Full Barb Equals 10 m/s.

Top Left: SAMPLE SIZE
Top Right: $\bar{V}_p$
Bottom Left: ΔV_p
Bottom Right: ΔV_N

Multiply ΔV_p and ΔV_N by $N^{-\frac{1}{2}}$ to get Standard Deviations of the Mean.

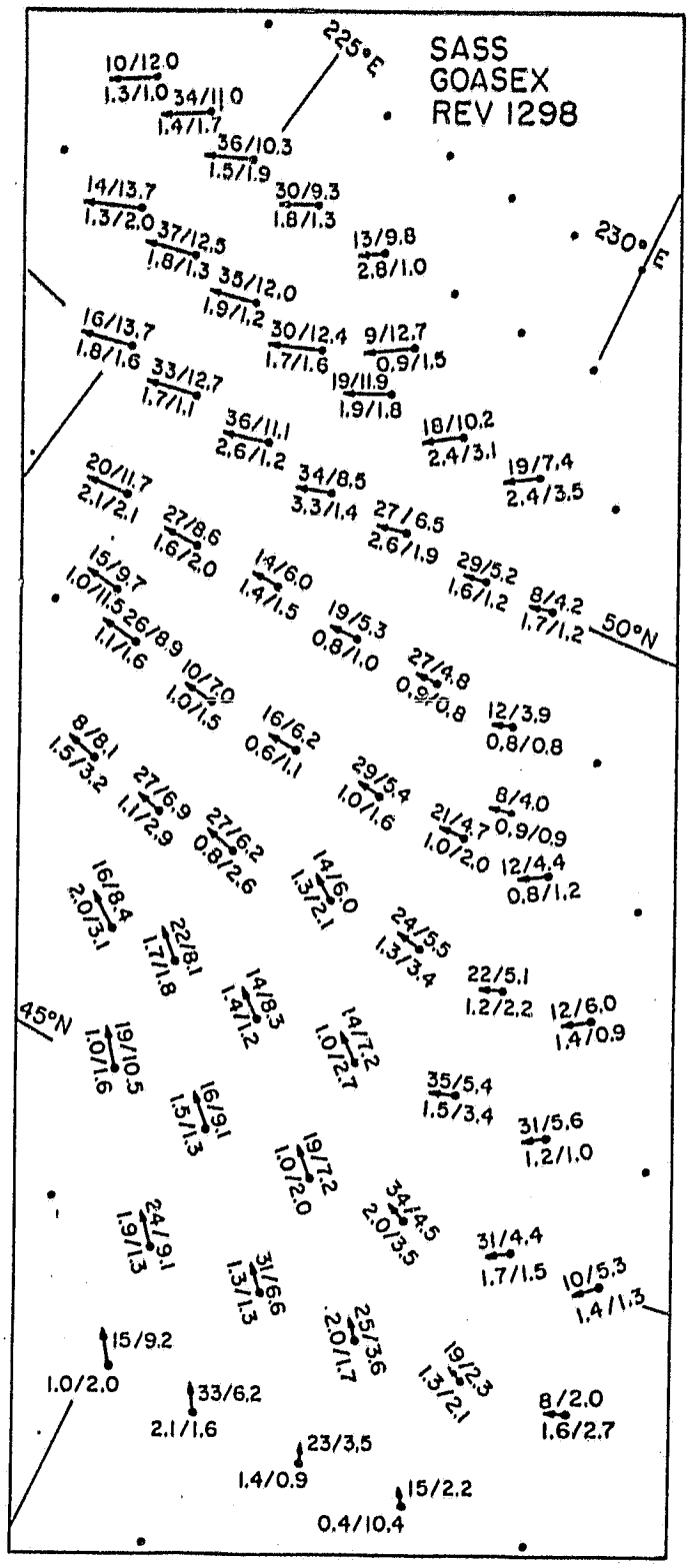

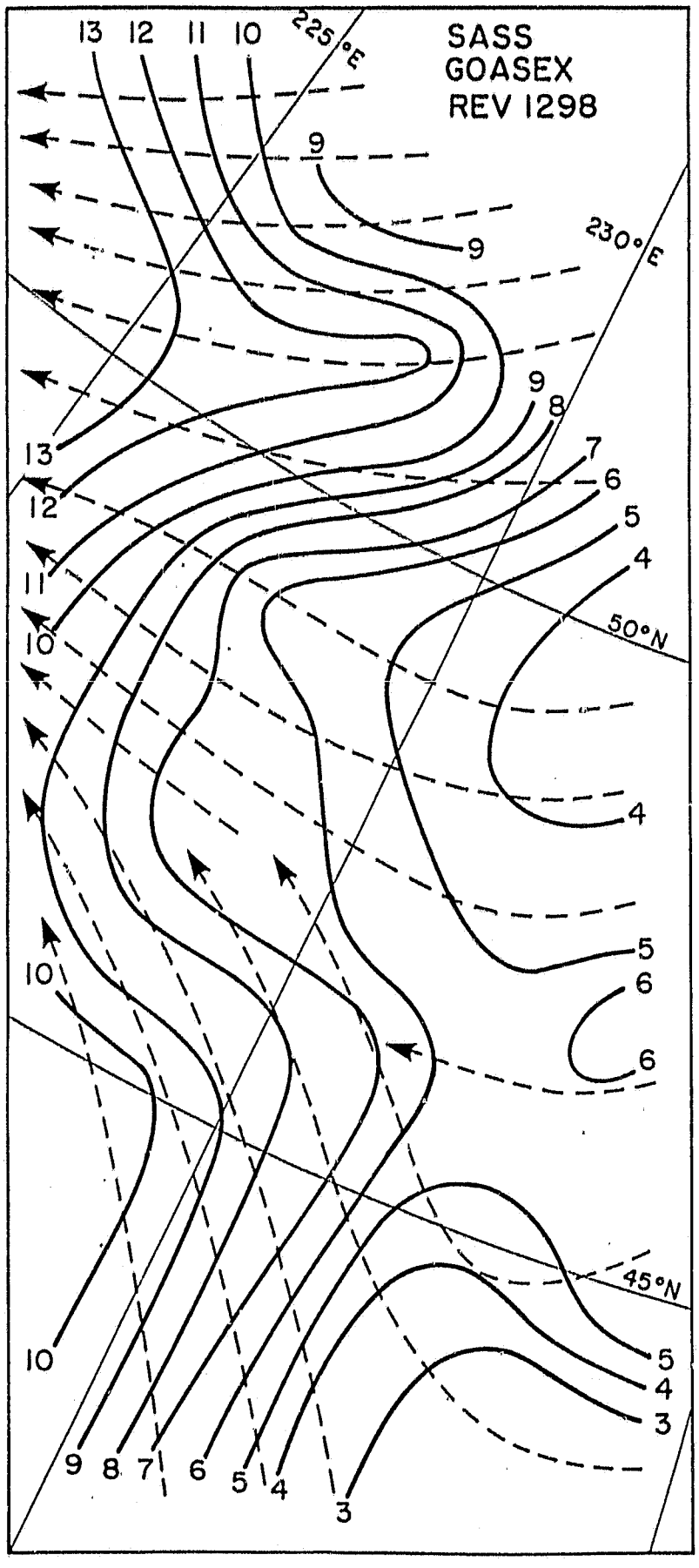

——— Solid Lines Isotachs

----- Dashed Lines Streamlines.

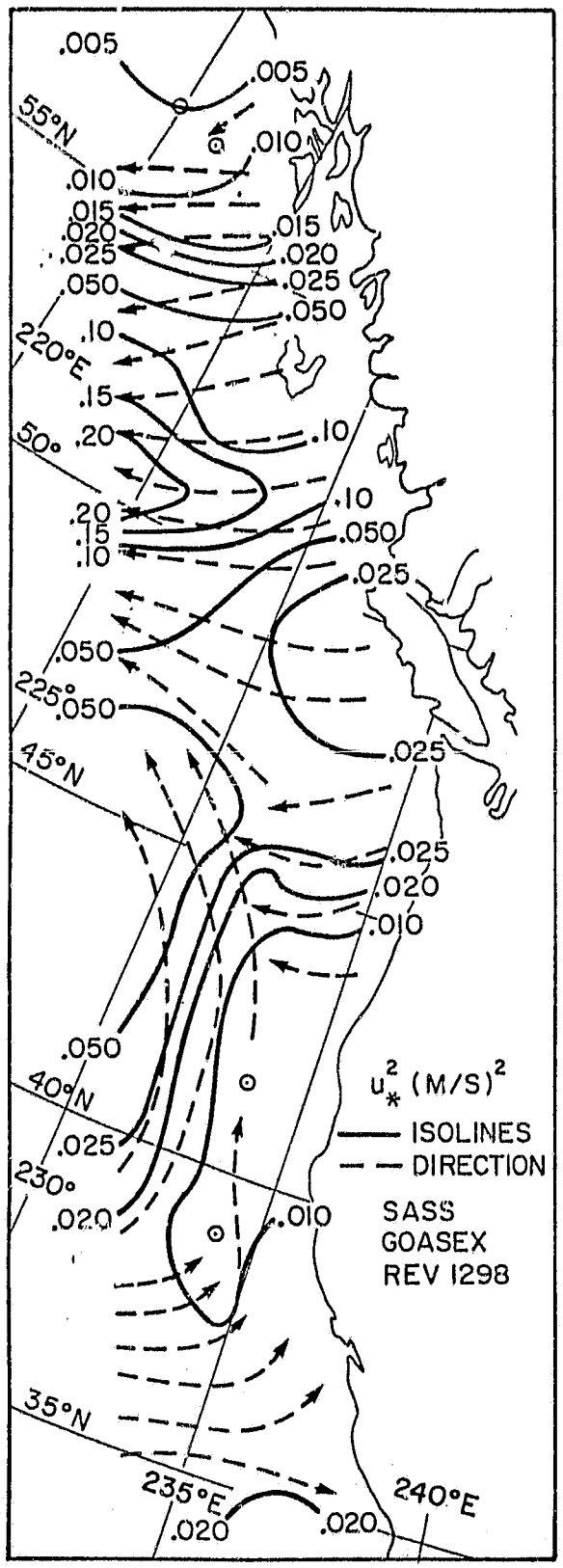

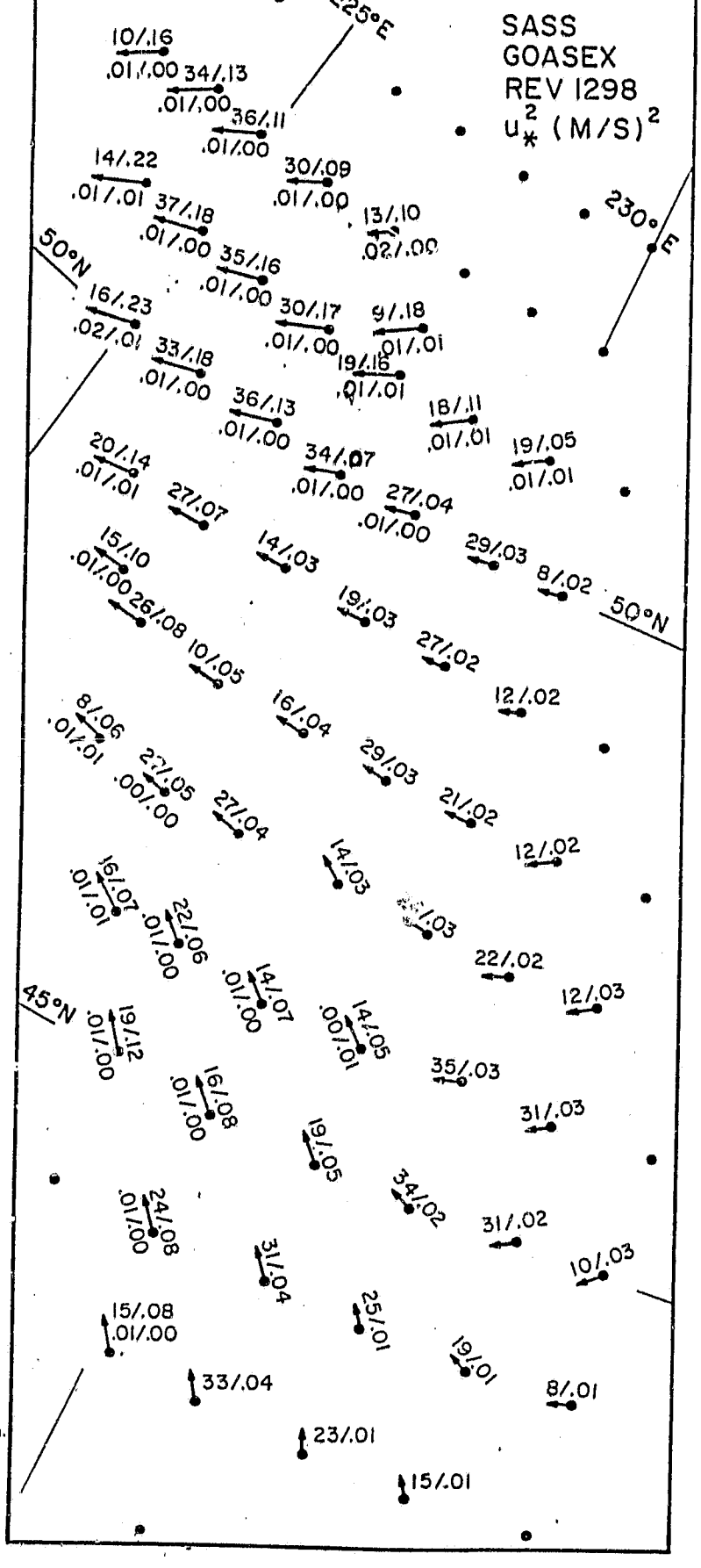

ORIGINAL PAGE IS
OF POOR QUALITY